1-2005

Polyaniline nanotubes: Catalysis and their conversion to carbon nanotubes

Stephen Paquette

Polyaniline Nanotubes: Catalysis And Their Conversion To Carbon Nanotubes

Stephen Paquette

July 2005

A Thesis Submitted In Partial Fulfillment Of The Requirements For The Degree Of

Master Of Science In Chemistry

Approved: Santhanam K.S.V.

Thesis Advisor

T. C. Morrill

Department Head

Department of Chemistry
Rochester Institute of Technology
Rochster, NY 14623-5603

Copyright Release Form

Polyaniline Nanotubes: Catalysis And Their Conversion To Carbon Nanotubes

I, Stephen Paquette, hereby grant permission to the Wallace Memorial Library, of RIT, to reproduce my thesis in whole or in part. Any use will not be for commercial use or profit.

Signature Stephen Paquette

Date 10/24/05

Table of Contents

Abstract

Polyaniline nanotubes, first synthesized by Parasarathy and Martin in 1994, have been studied extensively in recent years.[1] The study of these nanodimensional particles has been oriented mostly toward an attempt to understand the electrical and magnetic properties surrounding these semi-one dimensional objects and also toward applications for their utilization.[2] The ability to produce these nano-particles chemically but, without a template was first discovered by Wan in 1999.[3] The use of chemical oxidants often produces undesirable byproducts during the reaction. Therefore, we have used this as a launching point in order to first mirror this template-less synthesis in our lab and subsequently produce these same tubules electrochemically. Our in-situ doped polymer nanotubes showed identical spectroscopic and thermal characteristics as is shown in the original paper in which they were produced. Both optical and scanning electron microscopy were performed on the polymer nanotubes samples and both revealed the presence of tubules in large quantities.

The ability of these polymer nanotubes to produce a catalytic effect in the oxidation of aniline to form azobenzene was also investigated. This reaction was monitored by GC/MS and UV-Vis spectroscopy. The polyaniline nanotubes were found to exhibit a slight catalysis in this oxidation by suppression of byproduct azoxybenzene formation.

A different avenue was then taken in defining the changes which these polymers undergo upon heat treatment in different atmospheres. It was subsequently determined that the polyaniline nanotubes can be converted into carbon under an argon atmosphere. Furthermore, the conformational restriction provided by the parent polyaniline nanotubes

seem to offer a means by which carbon nanotubes can be preferentially formed when heated to 275°C. This was determined analytically by FTIR spectroscopy and energy dispersive X-ray analysis. Scanning electron microscopy was then again used to provide proof that single-walled carbon nanotubes are formed at 275°C and that multi-walled carbon nanotubes are formed at somewhere between 600-1000°C. These two allotropic forms of carbon are separated by a transition to glassy carbon occurring at 400°C.

Acknowledgements

Dr. KSV Santhanam, for his vision, patience, and guidance

My thesis committee, Dr. T.C. Morrill, Dr. L.P. Rosenberg, and Dr. M. Miri for their help and guidance.

The Department of Chemistry at RIT for financial support and research facilities.

Dr. S. Rommel of the Microelectrical Engineering Department at RIT for his amazing expertise in SEM imaging.

Dr. M. Illingsworth for shared equipment usage.

My wife, Van, my family, and my puppy, Homer—thank you guys I wouldn't have made it without your help.

Posters/Presentations

S. Paquette, Y. Xia, and K.S.V. Santhanam, **Template-Free Sythesis of Polyaniline Nanotubes by Electrochemical Polymerization**, Abstracts, 32nd Northeast Regional Meeting of the American Chemical Society, Rochester, NY, United States, October 31-November 3 (2004).

S. Paquette and K.S.V. Santhanam, **Synthesis and Catalysis of Polyaniline Nanotubes: High Temperature Conversion to Carbon Nanotubes**, presentation, 205th ESC meeting, Quebec City, CAN, May 2005.

List of Figures

List of Schemes

1. Introduction

Conducting polymers were first discovered in 1976 by Shirikawa, Heegar, and MacDiarmid.[4] A specific conducting polymer, polyaniline, has been extensively studied since the mid 1980s. Polyaniline, or PANI, has the attractive properties of being conductive yet, easily processed and durable. In 1994, micro- and nano-tubules of polyaniline were synthesized by Parasarathy and Martin using a alumina-silica template.[1] A template-free synthesis was subsequently reported in 1999 by Wan et al.[3] These nano-structured polymers are of great interest due to their semi-one dimensionality and their retention of conductivity.[5] The original methods for synthesizing these polymer nanotubes have not been largely improved upon since their original discovery. Therefore, it is the goal of this thesis to improve upon the synthesis methodology for creating conducting polymer nanotubes. This has been accomplished by initiating polymerization electrochemically and without the hindrance of a conventional template. An interesting and potentially incredible discovery was also happened upon in characterizing the newly produced polymer nanotubes. Upon heating under an inert atmosphere the tubes could be carbonized while retaining their original dimensions—in effect to produce carbon nanotubes. It was found that the types of tubes produced, either multi-walled or single-walled, could also be selected for by variation of temperature and that single walled tubes could be produced at a much lower temperature than traditional methods allow for.

1.1 Conducting Polymers

Three types of conducting polymers are known: ion—polymer solid electrolyte systems, composites of electronic conducting materials in non-conducting polymers, and polymers that conduct electricity by electronic transport. In the classical sense, only the latter is thought of as having an inherent conductivity. The conductivity observed in these macromolecules results from electron-hole transport. Electron-hole transport is simply the transfer of electrons localized on a particular atom in a macromolecule to an adjacent atom either in the polymer chain or in an adjacent macromolecule which is spatially close enough for transfer to occur. This provides a conduction path through the material, somewhat resembling electronic conduction in metals and semi-metals, which gives rise to the macromolecule's ability to conduct electricity.[6] The discovery of conducting polymers is important because their study has opened the door to understanding both the chemistry and physics of π-bonded macromolecules, it has allowed quantum physicists to address the question of whether or not alternation of bonding occurred in long chain polyenes as well as to ascertain the relative importances of electron-electron interaction versus electron-lattice interactions in macromolecules, they allowed for condensed-matter physics to be expanded by investigating the Pierls Instability (the idea that one dimensional conductors cannot exist), and finally—and possibly most importantly—allowed for the possibility of creating a new generation of conductors with variable conductivity, mechanical stability, and ease of manipulation inherent to polymeric materials.[4]

1.2 Polyaniline

Polyaniline is a conjugated macromolecule which can be black, dark green, or blue-violet depending upon oxidation state. It has been known for greater than 100 years and was known as "aniline black" or "emeraldine."[6] It is generally known in four different forms: leucoemeraldine which is insulating and blue in color, emeraldine base which is green and semi-conducting, emeraldine salt which is also green yet more conductive than emeraldine base, and pernigraniline which is violet or black and a strong insulator.[7] The electrical properties of polyaniline were largely unknown until the mid 1980s. Alan MacDiarmid first rendered the polymer conducting via two independent routes: oxidation of the leucoemeraldine base or protonation of the emeraldine base by acid-base methods.[8] This particular route involves modifying the oxidation state of the polymer by introduction of inorganic salts to generate the conductive state. This process is shown reversibly in Figure 1 below.

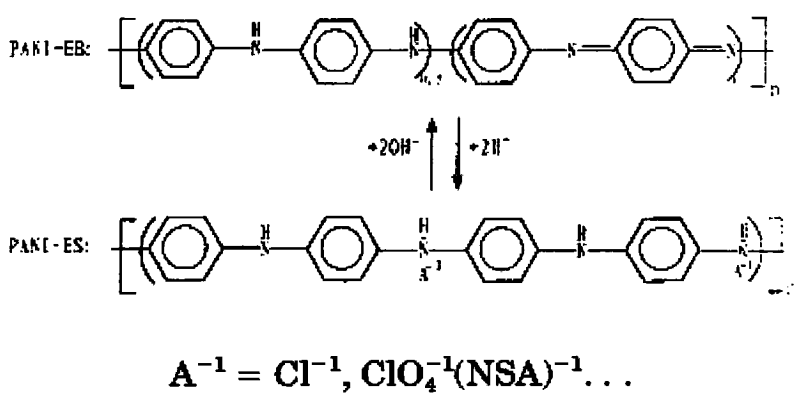

Figure 1. Emeraldine base interconversion. The conversion of emeraldine base to emeraldine salt by modification of dopant counterion. A^{-1} = counteranion.[3]

Though this process renders the polymer conducting, it did not render it easily processed. This problem was countered in 1992. Cao, Smith, and Heeger utilized a functionalized protonic acid to convert polyaniline to the metallic form and simultaneously allow for the polymer to be solublized in organic matrices.[9] The protonic acid in this process acted as a surfactant in that it formed a semi-micellar environment for the polymer in which a charged head-group acted to solvate the polymer and the hydrophobic tail group would solvate the complex in the surrounding solvent. This allowed for polyaniline to be made more easily accessible and therefore able to be used in forming different polymer blends.[10] These blends were also melt-processable so that they were now also available for industrial applications.

From these melts, a new method of creating polymer-based electronics emerged. The surfactant counterions seemed to allow the polyaniline to self-aggregate within the melt of the other polymer. Interestingly, when the support matrix polymer was removed, the polyaniline network was still conductive. This retention of conductivity allowed for new electronics possibilities, including the first light-emitting diodes, and is one of the major reasons that conducting polymer research holds so much potential.[11]

1.3 Polyaniline Nanotubes

Polyaniline was one of the first polymers to be structurally controlled on the nanoscale (made into nanotubules). They have attracted attention recently because of their unique properties and and potential applications in nanodevices.[11-14] Some of these properties include, single nanotube conductivity higher than that of the bulk polyaniline polymer, size which can be varied from 1-40 μm, conductivity which is

variable upon dopant counterion.[15] The list of current possible applications ranges from electrochromic devices, light-emitting diodes, chromatography, secondary batteries, electrostatic discharge protection, to corrosion protecting paint.[16-18]

1.3.1 Template Assembly Synthesis

The first polyaniline nanotubes were synthesized in 1994.[1] In this synthesis, a porous alumina-silica template was used to provide a support for conformational control in directing nanotube growth. Monomer is injected into the pores and an electrical potential is applied to the complex. Monomer is oxidized to form the polymer inside the porous network which then adopts a tubular conformation as the polymerization goes to completion due to the spatial constraints of the template. This method produces neat polymer tubules however, its utility is limited due to the clean up steps required to remove the alumina-silica template.

1.3.2 Self-Assembly Synthesis

This was the synthesis of choice until 1999 when Wan et al. developed the first template free synthesis.[3] This synthesis produces polyaniline nanotubes from solution. No traditional template is involved so no clean up steps are necessary. This synthesis has the added advantage of doping the polymer as it is synthesized. This is accomplished by using a surfactant to provide a network for the tubules to form in. This surfactant doubles as the dopant and produces conductive polymer directly. The polymer nanotubes produced by this method are not neat however, as is the case in the template synthesis

method, and the percentage of tubules produced is greatly surfactant/monomer ratio dependant.

1.4 Formation Mechanism

As mentioned earlier, there exist two alternative methods for polyaniline nanotube formation, the template method and the template-free method. This section will discuss the advantages, differences, and mechanistic aspects of these two methods.

1.4.1 Template Assembly

In template synthesis of polyaniline nanotubes, nanostructured polymer is formed using an electric current to initiate polymerization within the channels. Kinetics done by Dong et al. 2004 suggest that tube formation during polymerization is caused by single chain monolayer crystallization and then later by diffusion controlled polymerization.[19] X-ray diffraction also showed that the electrosynthesized polyaniline was composed of both crystalline and amorphous polymer indicating that the final structure is not continuous. The formation of polyaniline nanotubes by electropolymerization in a template is currently thought to follow the same formation kinetics as the electrocrystallization of metals. In this model, a nucleation site serves to initiate crystallization and crystallization then continues in either 2D progressive, 2D instantaneous, or 3D progressive fashion.[20] Of these, the 2D instantaneous and 2D progressive models appear to dominate due to the spatial restraints imposed by the template. Not much is currently known beyond this concerning the mechanism of polyaniline nanotube formation in a template.

1.4.2 Self-Assembly

The template-free formation of polyaniline nanotubes occurs by a different mechanism than that of template formation. Firstly, the "template" which is used to form the tubules is formed by micellar aggregation. In this process anilinium salt monomer and the surfactant form micelles at concentrations exceeding the critical micelle concentration of the surfactant. The micelle formed may be selected for by varying the ratio of monomer/surfactant. The micelles then aggregate with each other to form micellar bodies which are tubular. Polymerization is then initiated and the polymer tube is formed. This process is diagrammed in Figure 2 which shows 4 different outcomes possible from different amounts of surfactant present during synthesis. In micelle A, anilinium salt, labeled (+)~~~~ , is present in the exterior of the micelle along with the surfactant, labeled (-)~~~~ . In this aggregate, no aniline monomer is present on the interior of the micelle. Therefore when synthesis begins, the micellar aggregate contains no aniline on its interior resulting in the formation of a tubule. In micelle B, monomer has reached the micellar aggregate interior resulting in rod formation when polymerization is initiated. In micelle C, no surfactant is included in the reaction. Anilinium salt acts as a surfactant so it serves to produce its own template upon reaching the critical micelle concentration and at low pH. Again however, the same trend is repeated with tube formation occurring when monomer is excluded from the aggregate interior and rod formation occurring (micelle D) when monomer is included in the interior.

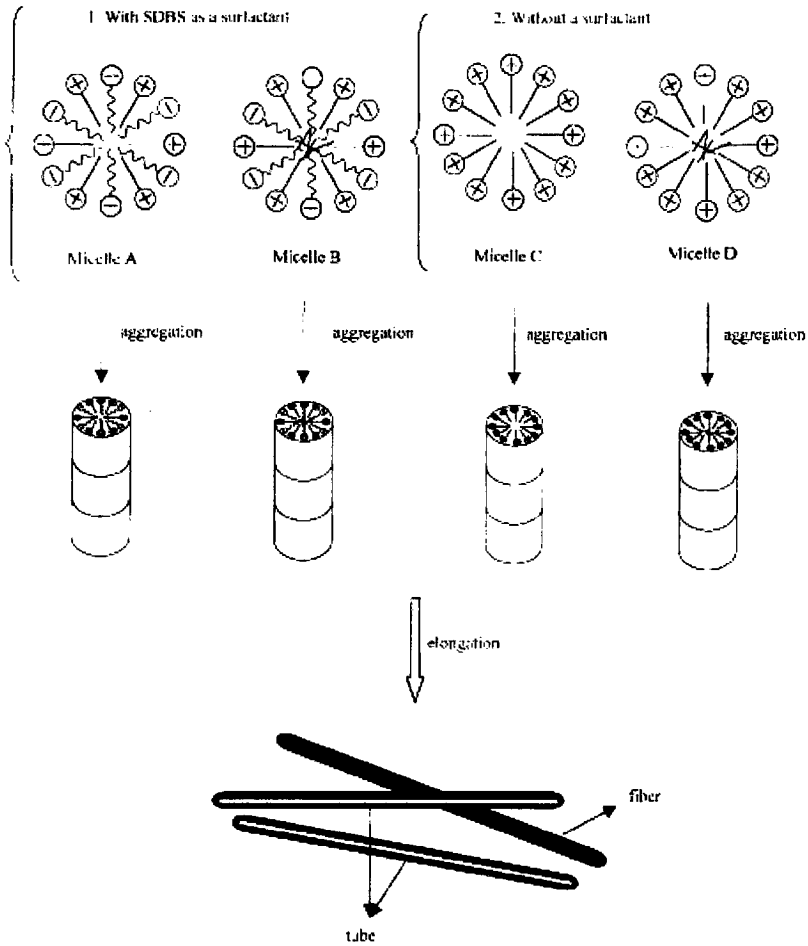

Figure 2. Mechanism of template-free nanotube formation. Formation of polyaniline tubes or rods can be selected for using the template-free synthetic method.[30]

The actual mechanism is also different in that the entire tubule is homogenous with respect to structure. This was shown by Yang and Wan in 2002 in which chiral polyaniline nanotubes were formed using camphor sulfonic acid as the dopant/surfactant.[21] These tubes were then found to exhibit Cotton effect when analyzed using circular dichroism. Cotton effects are indicative of helical structures therefore, this showed that polyaniline nanotubes formed by template-free methods adopt the conformation of a helix.

It is also impossible for the same mechanism of formation to occur by this method since there is no actual foundation for crystal nucleation to occur upon. Translational motion of micellar aggregates does not provide a "solid" support in this sense. Instead, the timescale on which the polymerization occurs is what actually allows for a 3-dimensional structure to be selected for during synthesis. Radical lifetimes in polymerizations are on the scale of nanoseconds.[22] The translational motions which micelles undergo are predicted to be on the same time scale but, for aggregates such as those formed in these emulsions each micelle rotation must be averaged over several thousand component micelles so the aggregate structure appears to be somewhat static when compared to the polymer chain propagating radical.[23]

1.5 Carbon Nanotubes

It would be difficult to discuss any aspect of nanostructured materials properly without making reference to the material that really started the whole revolution of nanoscience—the carbon nanotube. Carbon nanotubes were first isolated by Sumio Iijima in 1991.[24] These were first isolated by an arc-discharge synthesis method which is diagramed in Figure 3. In this method, nanotubes are synthesized at the end of a carbon cathode which is stationary. The anode is placed on a moving drive and slowly moved toward the cathode as carbon is used up in order to keep the electric arc constant. The soot produced as well as the carbon which is deposited on the cathode contain carbon nanotubes.[25]

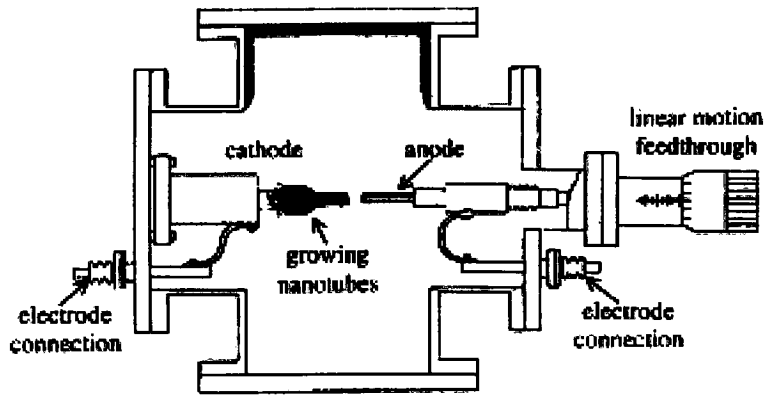

Figure 3. Arc-discharge apparatus for synthesis of carbon nanotubes.[25]

The original tubes were found to be helical in a fashion with diameters ranging from a few nanometers to a few tens of nanometers. They can exist as either zig-zag or armchair configuration as shown in Figure 4 or as a chiral wrap. Chirality is the major

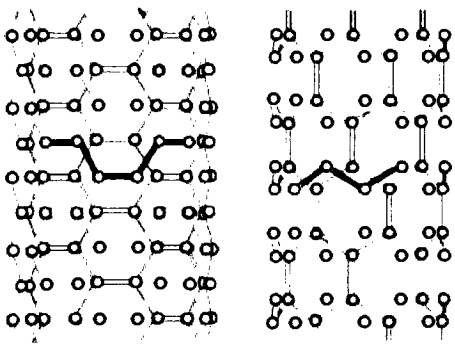

(a) (b)

Figure 4. Different conformations of carbon nanotubess. (a) Armchair conformation of carbon atoms in carbon nanotube. (b) Zig-zag conformation of carbon atoms in carbon nanotube.[25]

determinant in how intrinsically conductive the carbon nanotubes are.

Carbon nanotubes have many properties which are the impetus for the intense research initiative into their synthesis and utilization. Some of these properties are

extreme elasticity with a Young's Modulus of greater than 1 TPa[25], the highest current density of any known material at 10^8 A/cm[26], as well as being roughly 100 times stronger than steel.[26] Therefore, it is interesting to see what parallels can be made between carbon and conducting polymer nanotubes and whether or not there is a method of interchanging one for another.

1.6 Polymer Carbonization

Only very recently has there been any investigation into controlled carbonization of polymer compounds. This has taken place primarily in Japan although there is some promising research going on in the United States as well. Of the different carbonization methods, pyrolysis of polymer blends to form mesoporous carbon, pyrolysis of organic gels prepared by sol processes, template carbonization, even catalyst mediated carbonization into structured moieties.[27] Carbon nanotubes have recently been produced from carbonization methods without the use of a catalyst. This was done by Kim et al. in 2001.[28] Strangely this was not fully investigated until very recently (2004-2005). In this paper, poly(para-phenylene vinylene) nanotubes were synthesized in a template. These polymer tubules were then heated to 1000°C in an inert atmosphere. They noted that elemental analysis showed only carbon, which only really confirms that Argon gas was not incorporated into the material, and that an increase in the amount of crystalline π-character in the material which is characteristic of carbon nanotube formation. The idea of using a template inherent to a polymer nanostructure to form a carbon nanostructure has only been investigated in the original laboratory which reported it.

1.7 Purpose of the Thesis

The purpose of this thesis is three-fold. Firstly, to improve upon the template-free synthesis of polyaniline nanotubes. The original synthesis by Wan et al.[3] as earlier stated has not been largely improved upon and still does not synthesize polymer nanotubes as a neat material. Electropolymerization holds great promise in this aspect as there is a local synthesis at the working electrode. Local environments are more easily manipulated than a large scale environment. Additionally, the local environment could be altered to select for tube formation, such as modifying the electrode to be more conducive to tube formation. Moreover, washing the electrode is very easy to do whereas cleanup of a bulk synthesis is more laborious due to the presence of more material.

Secondly, the oxidation of aniline to form azobenzene in the interior of the polyaniline nanotubes will be examined. This has already been done using functionalized carbon nanotubes by Gordon, et al.[29] However, the relationship between tube diameter and catalytic rate were of interest since polyaniline nanotubes are roughly 10 times larger in diameter than functionalized carbon nanotubes.

Thirdly, we will investigate the conversion of polyaniline nanotubes to carbon nanotubes. Carbon nanotubes hold great potential in many different areas as noted earlier. Polyaniline nanotubes also hold great potential. It is of interest to see what possibilities interconverting these two materials may hold.

2. Experimental

2.1 Chemicals

Aniline (Aldrich) was purified by distillation and collected at 180°C and kept under refrigeration. Reagent grade 2-Naphthalenesulfonic acid was procured from Fluka. Azobenzene was purchased as crystalline solid from Aldrich and dessicated. Ammonium persulfate was purchased from Aldrich and used as received. Hydrogen peroxide (30% vol/vol) (Baker Analytical grade) was kept under refrigeration. All solvents were used as received. Fisher Scientific decolorizing carbon (Norite) was used as the active carbon sample. All chemicals were of reagent grade. Solvents were of HPLC grade except for distilled water.

2.2 Instrumentation

The RIT Chemistry Department provided all needed instrumentation with the exception of EDX analysis (outside contract) and SEM imaging (RIT Microelectronic Engineering Department).

2.2.1 Cyclic Voltammetry

Cyclic voltammetry curves were taken using Gamry Corrosion Cyclic Voltammetry software. Working electrodes consisted of Pt plate, Pt wire, or indium-tin oxide (ITO) enriched plastic. A graphite rod was used as the counter electrode and potential was measured against a saturated calomel electrode.

2.2.2 UV-VIS Analysis

All UV-Visible spectra were taken using a Shimadzu High Resolution UV-2401 spectrometer. A 1 cm x 1 cm x 10 cm quartz cuvette cell was used as the sample holder with the following method parameters: 200-1000 nm scan, slit width of 0.5 mm, and medium scan speed. All measurements were measured against acetonitrile solvent.

2.2.3 GC/MS Characterization

Azobenzene conversion was measured on a Hewlett-Packard 6890 GC with a 5973 Mass Selective Detector. An Agilent 19091S-396 60 m x 250 μm x 0.25 μm column was used for these quantitations. Injection manifold was held at 280°C with a column temperature ramp program of 150°C-320°C at a rate of 20°C/min. Sample injection volumes were 1 μL in all experiments.

2.2.4 FTIR Characterization

All infrared spectra were taken using a Biorad Excalibur FTIR FTS3000 with Diffuse Reflectance cell. Scan parameters were as follows: 2 cm^{-1} resolution, 4000-400 cm^{-1} scan range, medium scan speed, and 64 scan averaging.

2.2.5 TGA Characterization

Thermal gravimetric measurements were taken using a TA (Delaware) Instruments TGA 2050. Platinum pans were used for measurements above 600°C. Either nitrogen or compressed air were used as carrier gas as specified. All scans were taken at 10°C/min scan rate.

2.2.6 Polarizing Microscopy

Optical microscope images were taken using a Reichert-Jung Scope with video imaging. All images were taken using reflective light and no filtering. Magnification of 100 X or 500 X was used as specified.

2.2.7 SEM Imaging/EDX Analysis

All scanning electron imaging was done with the help of Dr. Sean L. Rommel of the Microelectronic Engineering department at RIT. Imaging was done at varied magnification with 20kV beam current, 0.6 pA filament current, and 0°C stage temperature. EDX analyses were performed by an outside contracted group using their SEM/EDX instrument.

2.3 Procedures

2.3.1 Chemical Synthesis of Polyaniline Nanotubes

Chemical synthesis of polyaniline nanotubes was carried out at 0-4°C with stirring. Ammonium persulfate (0.1 M) was used as radical initiator along with an equimolar concentration (0.1 M) of distilled aniline monomer. This reaction was carried out for 15 hours in 0.1 M HCl and (0.4 M) 2-naphthalene sulfonic acid. Polyaniline nanotubes were recovered in bulk by vacuum filtration followed by 3 washes each of water, ethanol, and diethyl ether. Product was allowed to dry for 24 hours prior to analysis. Polyaniline control was synthesized using the same process but excluding surfactant.

2.3.2 Electrochemical Synthesis of Polyaniline Nanotubes

Electrochemical synthesis of polyaniline nanotubes was carried out at 0-4°C with stirring. Working electrode (Pt plate, Pt wire, or ITO plastic) was utilized for radical generation and 0.05 M final conc. of distilled aniline monomer was used as substrate. This reaction was carried out for 2 identical scans at 10 mV/s scan rate and from 0 mV to 900 mV scan range. This polymerization was carried out in 0.1 M HCl and 0.2 M 2-naphthalene sulfonic acid. Polyaniline nanotubes were recovered as deposited on the working electrode. Product was washed in 0.1 M sulfuric acid and deionized water and allowed to dry prior to analysis. Polyaniline control was synthesized using the same process but excluding surfactant.

2.3.3 Catalytic Conversion of Aniline to Azobenzene

Distilled aniline (0.1 M) was reacted with 30% H_2O_2 (0.1 M) in acetonitrile for 60 minutes with UV-Vis spectra taken every 5 minutes. Polyaniline nanotubes were added as catalysts in 40 mg amounts. These were measured against normal polyaniline and unfunctionalized multi-walled carbon nanotubes as well as uncatalyzed controls. These reactions were performed at room temperature.

2.2.4 On-Column Conversion of Aniline to Azobenzene

Polyaniline nanotubes were used as packing material for an on-column conversion experiment (sealed with glass fiber). A control of glass fiber was used to compare the sample column to. Distilled aniline (0.1 M) was reacted with 30% H_2O_2 (0.05 M) in acetonitrile and instantly drawn over the column. The reaction mixture was passed over

the column 3 times in both control and active column. Results were qualified and quantified by GC-MS.

2.2.5 Thermal Conversion of Polyaniline Nanotubes to Carbon Nanotubes

Polyaniline nanotube enriched samples (200 mg) were heated in an argon atmosphere to 275°C, 400°C, and 1000°C. The sample remains after heating were recovered and weighed using an analytical balance. These samples were then analyzed by EDX, SEM, TGA, and optical microscopy.

3. Results and Discussion

3.1 Chemical Synthesis of Polyaniline Nanotubes

Polyaniline nanotubes were chemically produced following the method of Wan et al. 1999 in which emulsifier acts as template and dopant[3]. The emulsifier/dopant 2-naphthalene sulfonic acid was combined with distilled aniline monomer in a 4:1 molar ratio. Ammonium persulfate was added as a free-radical initiator continuously over the course of reaction until completely dissolved. As stated in the experimental section, this reaction was carried out for 15 hours at 0-4°C. Reaction was terminated by washing with excess deionized water, ethyl alchohol, and ether. Polyaniline nanotubes were formed in the matrix of the parent polymer as a green bulk solid.

3.1.1 UV-Visible Spectroscopy

Polyaniline nanotubes were characterized by UV-Vis spectroscopy and compared to the original literature (shown in Figures 5 and 6)[3]. These spectra were taken as a dispersion of polyaniline nanotubes dissolved in dimethyl sulfoxide (DMSO). In the original synthesis, the UV-Vis absorption spectra were taken and showed peaks at 880 nm, 640 nm, and 396 nm. The same product was then dedoped by allowing the tubules to sit for 24 hours in DMSO shown in Figure 6. This was not done in the original paper however, it is useful as a method of depicting the conductivity of the polymer nanotubes as well as their stability in solution.

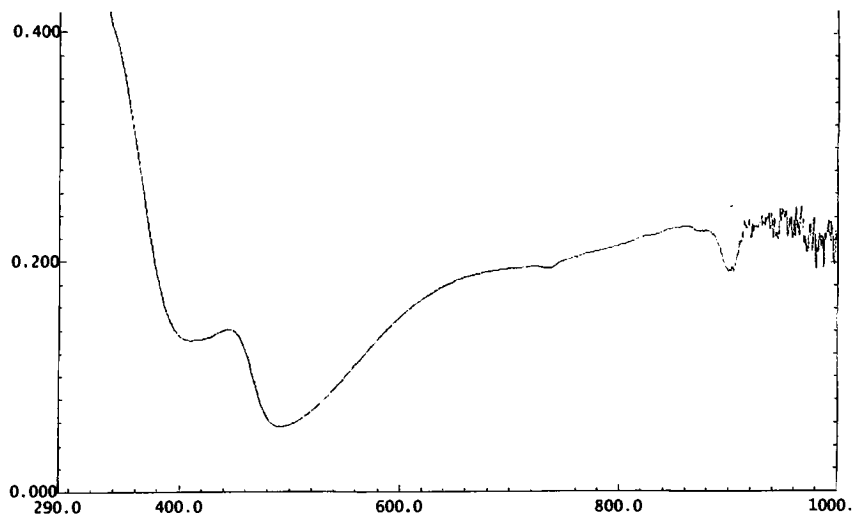

Figure 5. Visible spectroscopy of doped polyaniline nanotubes. Absorption spectra of 2-naphthalene sulfonic acid doped polyaniline nanotubes.

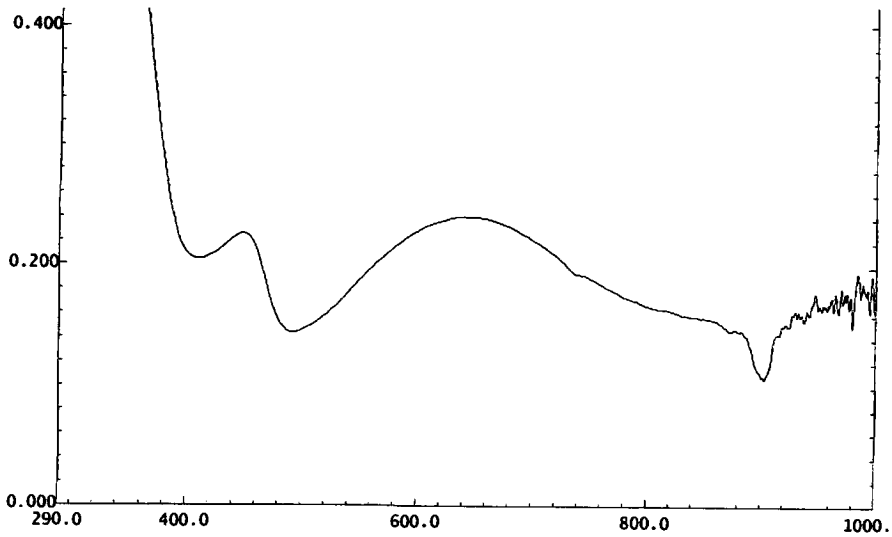

Figure 6. Visible spectroscopy of de-doped polyaniline nanotubes. Absorption spectra of 2-naphthalene sulfonic acid de-doped polyaniline nanotubes.

In the case of in-situ, or during-synthesis, doped polyaniline nanotubes clear indications of conductive regimes are present in the UV-Vis spectra. These conductive regimes are known to be present due to the absorption bands present at 400 and 900 nm. The absorption bands at 400 and 900 nm are characteristic of a conductive state.[31] To form this conductive state, dopant ions are necessary and act to create conduction by forming polarons. Polarons are, for clarity, paired electons on the same carbon adjacent to an unpaired electron which resides between the conduction band and the ground state. They are a necessity for conductance in a molecular conductor. This is shown below in scheme 1 along with bipolarons and solitons—other excited energy states possible for conductive electrons. The bands at 900 nm are those belonging to the bipolaron bands with the band at 600 nm in the dedoped state being that of a polaron band. Polarons are formed in the undoped material more prevalently due to the absence of the dopant which facilitates exciton formation. Polarons are inherent to molecular conductors and are only

less populated when a dopant ion is present to stabilize bipolaron and soliton pair formation. The band at 400 nm is that of the π->π* transition observed in the aromatic rings which is why it is conserved for both spectra.[31]

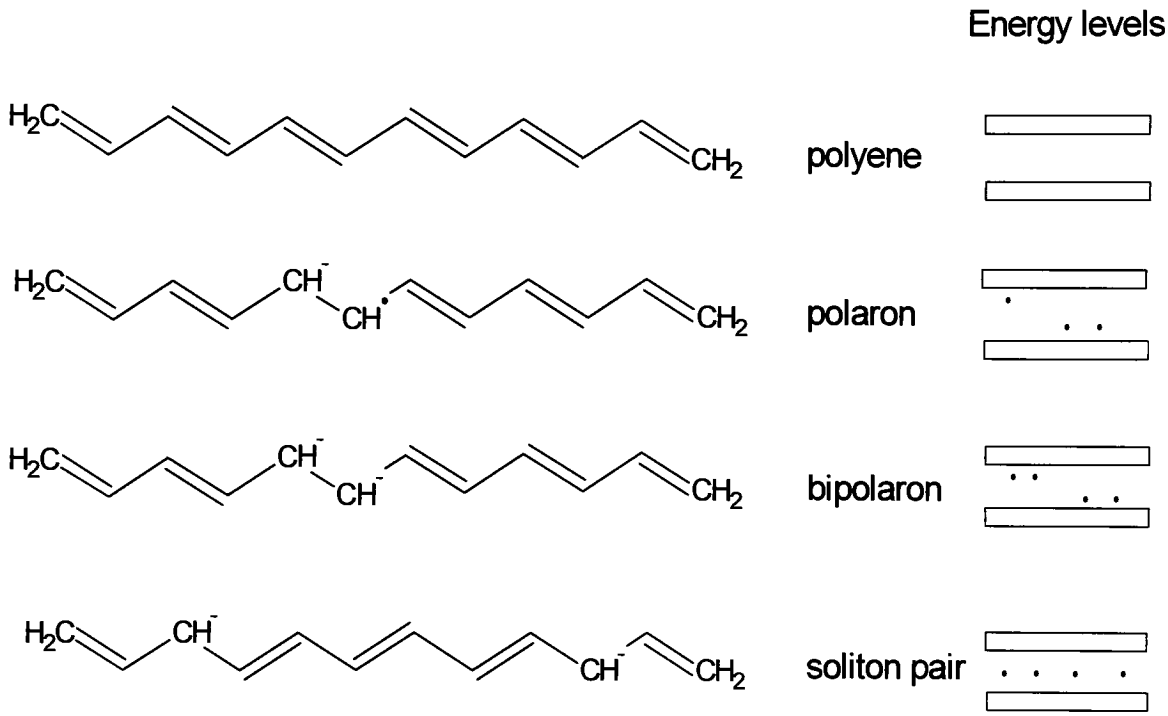

Scheme 1. Exciton states in doped/conducting polyene macromolecules. Energy levels depicted at right show ground state (lower bar) and conduction band (upper bar) energy levels. The dots depict electron energy levels. Those which are dopant injected reside in the energy levels closest to but, not inside the conduction band. Those electrons associated with parent polyene chain conjugation tend to reside closer to but, not inside the ground state when sharing π-bond carbons. In the ground state polyene, all electron energy states are ground state levels.[6]

3.1.2 Diffuse-Reflectance FTIR Spectroscopy

The product of the emulsion reaction was then compared to the original paper by diffuse-reflectance FTIR. The original paper showed absorption bands at (label a) 1576

cm^{-1} and (label b) 1496 cm^{-1}, respectively, consistent with benzenoid and quinoid stretches for C=C bonds. The C=N stretch mode was observed at (label c) 1300 cm^{-1} and the quinoid stretching for the C=N=C bonding was observed at (label d) 1140 cm^{-1}. These peaks are also observable in the product of our reaction indicated by arrows in Figure 7 as well as a typically observed N-H stretch at app (label f) 3000 cm^{-1}.

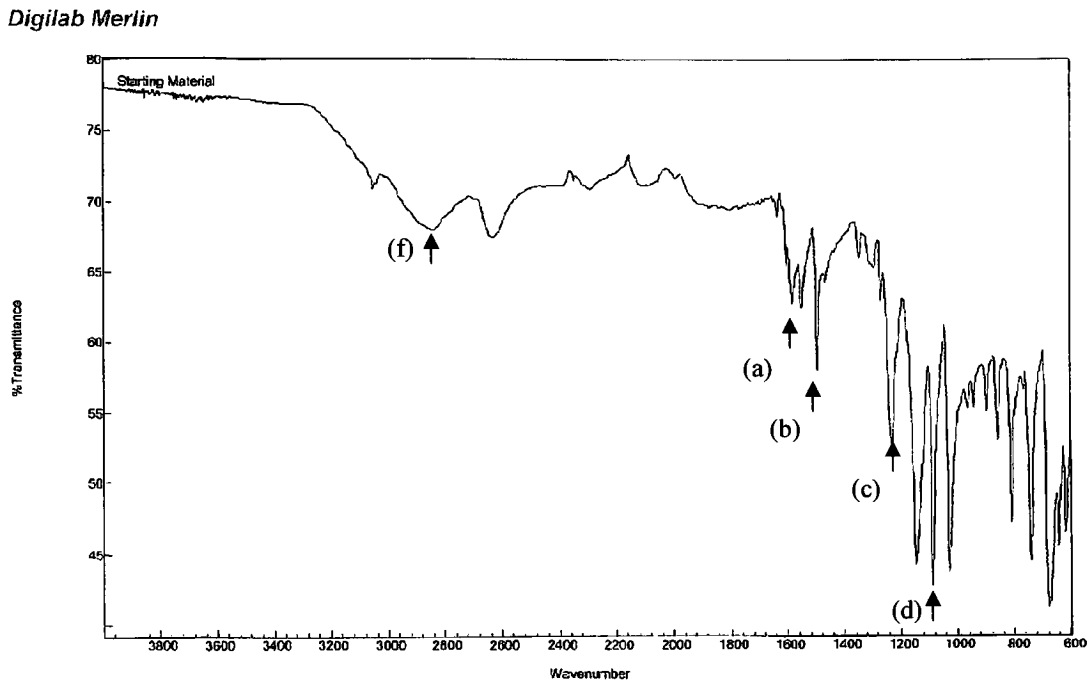

Figure 7. FTIR analysis of polyaniline nanotubes. Diffuse-reflectance FTIR scan of chemically produced polyaniline nanotubes. Labels a-f signify different infra-red absorbing moieties.

3.1.3 Optical Microscopy

Optical micrographs were taken of the products of the chemical reaction products. These images showed the presence of nanotubules in the reaction batches which were

emulsified and showed no tubule formation in the reaction batch lacking emulsifier. These photographs are shown in Figures 8-11.

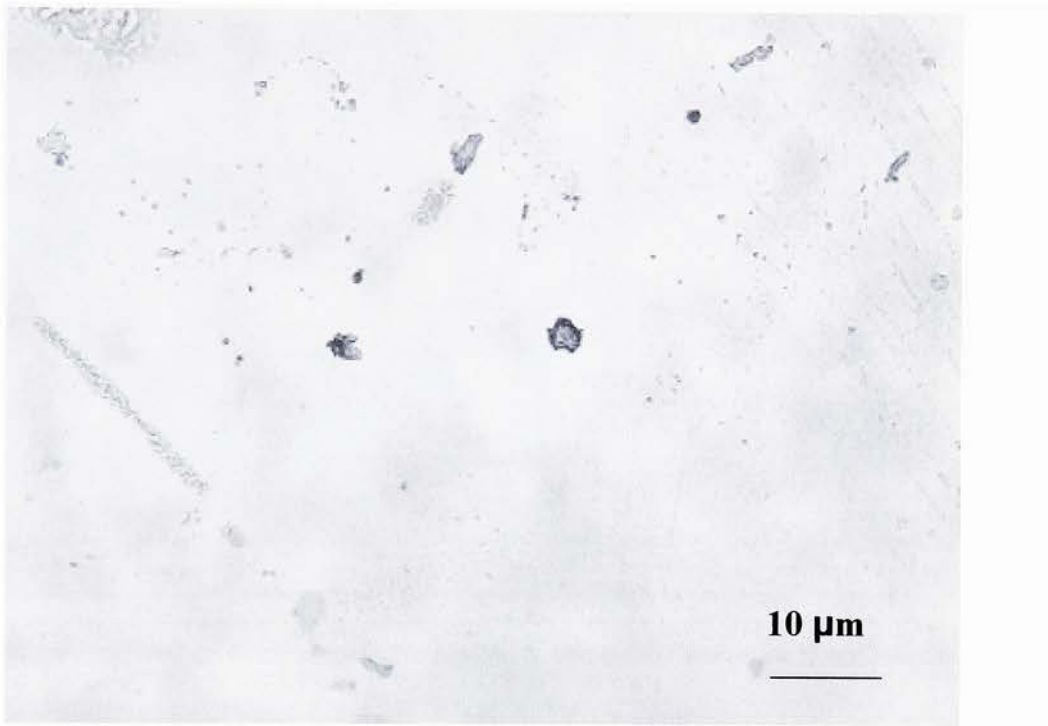

Figure 8. Polyaniline film produced by the chemical method.

Figure 8 shows a polyaniline film coated onto a glass slide. No bodies with apparent structure are visible throughout the film. The scale of the picture also s hows that the objuects which are not uniform with the rest of the film are smaller than the tubular bodies shown in the following figures 9-11.

Figure 9 shows a film in which surfactant was included in the synthesis. A possible tubular morphology is apparent in this film. At this point it remains to be proven whether or not the bodies are crystalline outgrowths from a focal point or actually polyaniline nanotubes. This is later addressed and proven by SEM imaging however, from this micrograph it can be seen that the sizes of the rod-like bodies observed are on the scale of 5-10 µm in length and less than 1 µm in diameter.

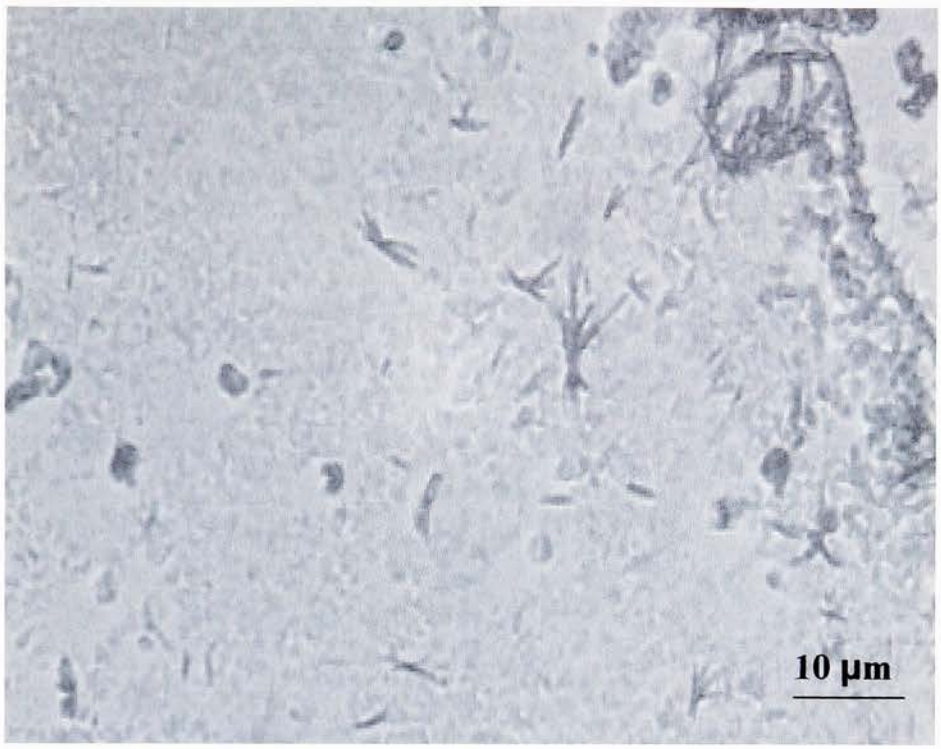

Figure 9. Template-free chemically produced polyaniline nanotube film. Polyaniline nanotube film chemically produced by a 1:1 molar ratio of emulsifier/monomer.

In Figure 10, the tubular bodies become longer and greater in number. Additionally, the question of whether a tube or rod is being formed can be somewhat addressed. The clusters show morphology with open interiors. These bodies are therefore, at least rods with open interiors. This could be an artifact due to the fact that this micrograph was taken using reflective light. Still at the very least it can be established that the shorter dimension to these bodies is round.

The presence of tubular morphology becomes more pronounced in figure 11. A cluster of tubules is visible with average dimension of <1 µm diameter x 40-50 µm length. Rods are also present to show the contrast between rods and tubes in this figure. The rods in this figure are darkly colored throughout whereas the tubes still appear to have

hollowed interiors. These tubes are much more distinctly formed than the previous micrographs show. This appears to be due to the surfactant/monomer ratio. This was also seen in the original description done by Wan et al.[3].

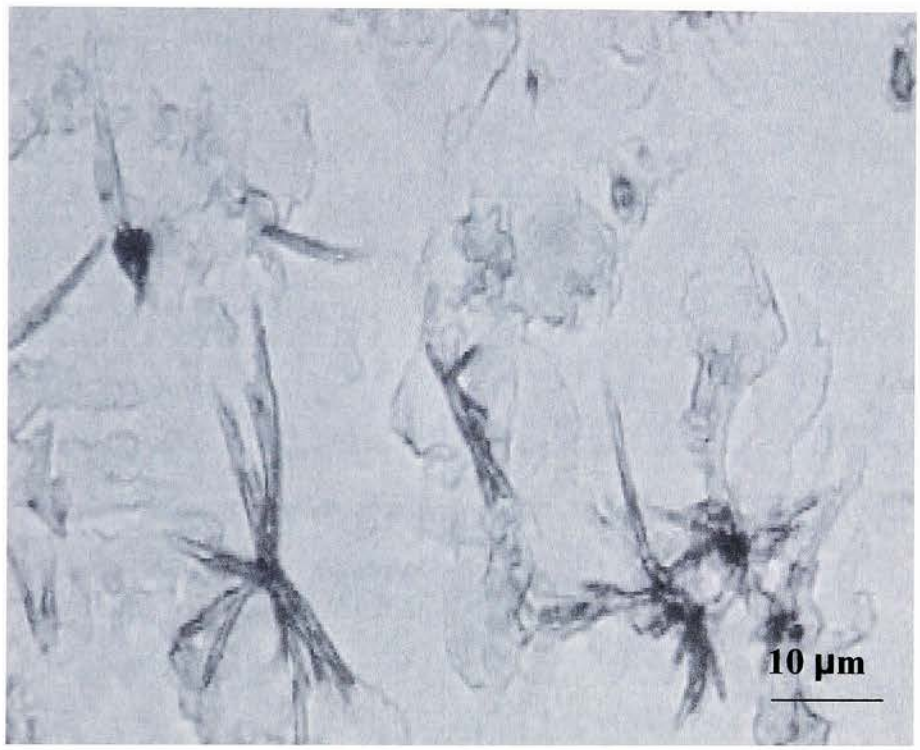

Figure 10. Template-free chemically produced polyaniline nanotube film. Polyaniline nanotube film chemically produced by a 3:1 molar ratio of emulsifier/monomer.

In summary, as the emulsifier concentration is increased from zero to 0.4 M, the tubular bodies produced seem to adopt a much more defined structure. Additionally, the tubes produced in the 4:1 emulsifier/monomer reaction seem to be longer than the ones produced at a 1:1 emulsifier/monomer ratio. In all cases, these tubes are formed within the parent polymer matrix.

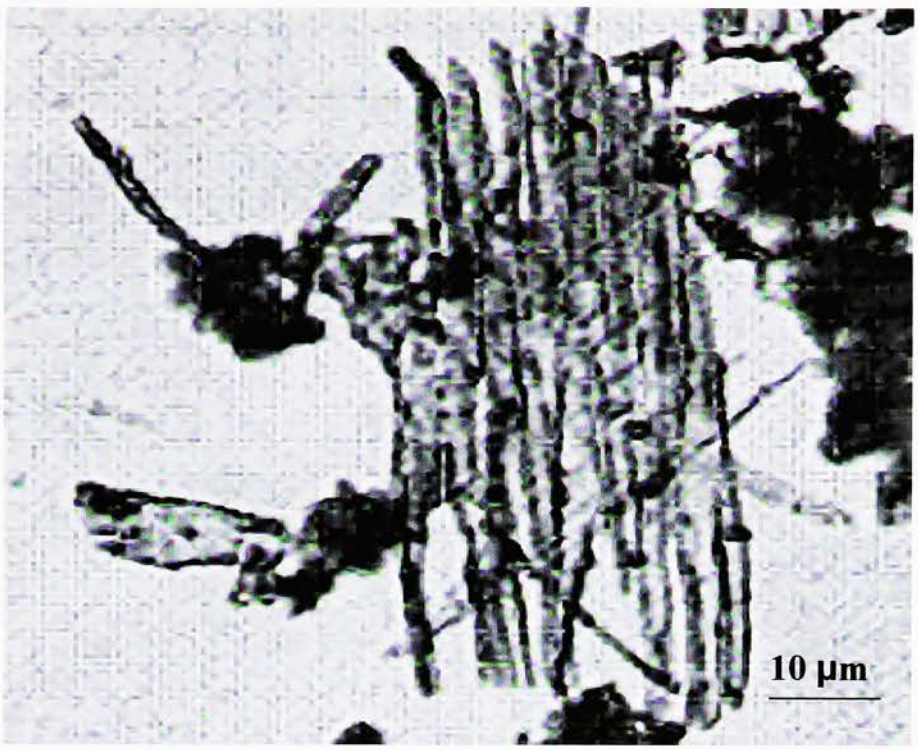

Figure 11. Template-free chemically produced polyaniline nanotube film. Polyaniline nanotube film chemically produced by a 4:1 molar ratio of emulsifier/monomer.

3.1.4 Scanning Electron Microscope Imaging

Figure 12 shows an electron micrograph taken of the 4:1 mole ratio reaction. In this image it is clearly shown that tubular morphology is present. Clear evidence of open ended structures is present as shown by the arrow (blue). Moreover, it can also be seen that these tubes which are produced are not necessarily rigid as they seem to be flexible enough to wrap around different areas of the amorphous regions. These results are in good agreement with those published by Wan, et al.[3] It is important to compare to the original paper in determining the guidelines for characterization. This is to prevent dissention among different labs as to whether or not tubes were established. This study

has been consistent with the original means of characterization as well as some additional means in order to be careful and consistent.

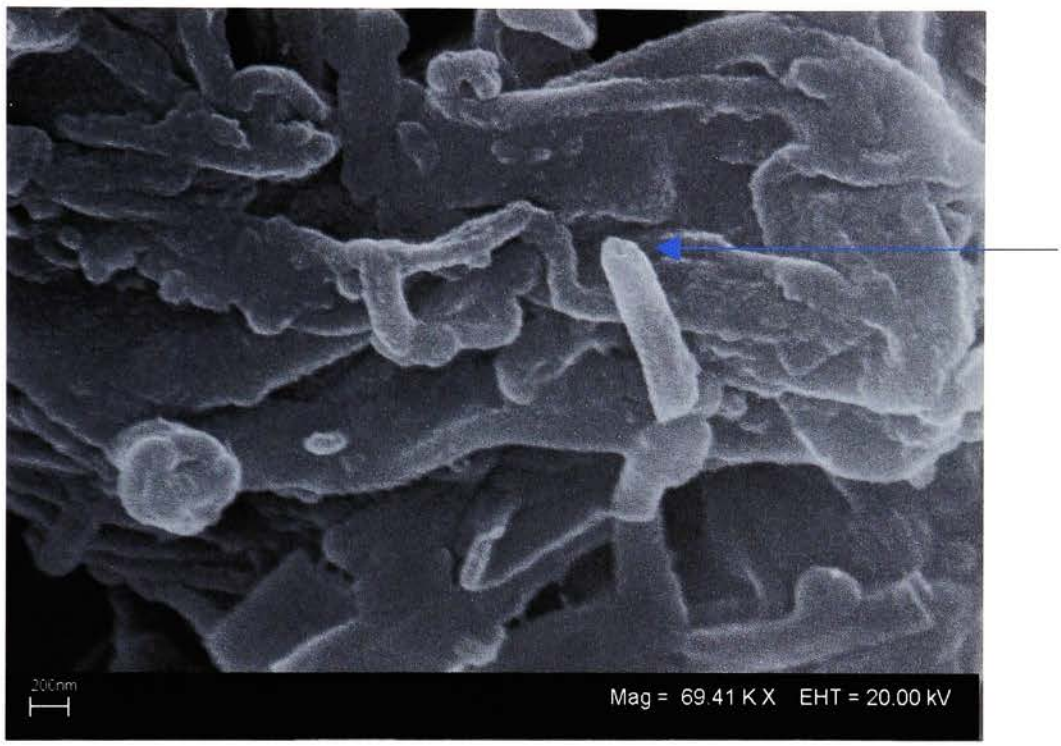

Figure 12. SEM image of 4:1 emulsifier/monomer chemical reaction product.

3.2 Electrochemical Template-Free Synthesis of Polyaniline Nanotubes

These results combined led us to believe that we had successfully synthesized polyaniline nanotubes in our laboratory. This then provided us with both a standard to compare new material to as well as a stepping point for pursuing more innovative research concerning polyaniline nanotube synthesis. Electropolymerization of poly aniline is thought to occur by Scheme 2, shown below.

In this depiction, the polymerization mechanism is identical to that of chemically initiated polymerization, the only difference being the source of the initiating radical.

This led us to the theorization that since the two initiation methods were mechanistically identical, they should both be applicable to polyaniline nanotube formation.

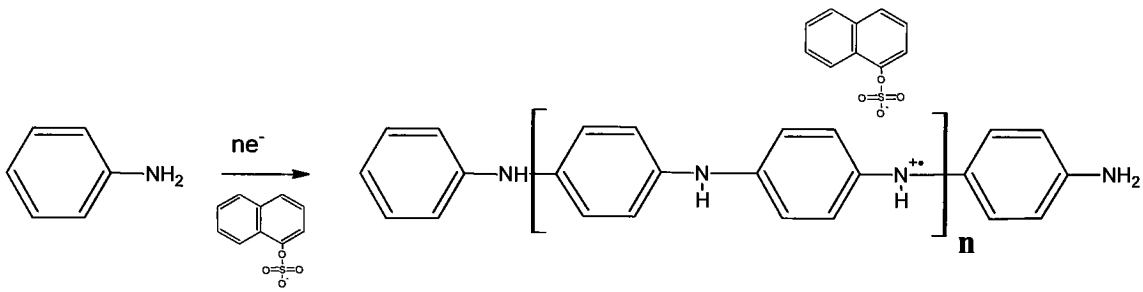

Scheme 2. Electropolymerization of polyaniline. In this scheme, 2-naphthalenesulfonic acid is used as dopant counterion and the quinoid form of the repeat structure is shown by the positive charge on nitrogen.

We therefore set out to synthesize polyaniline nanotubes by electrode-based initiation in an emulsified environment.

3.2.1 Cyclic Voltammetry

Cyclic voltammetry was used to polymerize distilled aniline monomer in emulsion medium on a Pt plate electrode. A control was also run in which no emulsifier was present. It can be seen in Figure 13 that a cathodic peak was present at approximately 700 mV indicating that reduction of anline monomer occurred when the reaction was run in 0.1 N H_3PO_4 medium.

The film produced by this method was then washed and characterized by cyclic voltammetry. The film was immersed in new 0.1 N H_2SO_4 and the potential swept from 0-1200 mV at 10 mV/s. The control for this experiment (electrochemically synthesized polyaniline on a Pt plate electrode) is shown in Figure 15 with the polyaniline nanotube

film shown in Figure 15. There are some remarkable differences between the two films. For one thing, the anodic peak observed in Figure 14 which is characteristic for polyanline oxidation occurs at 500 mV.

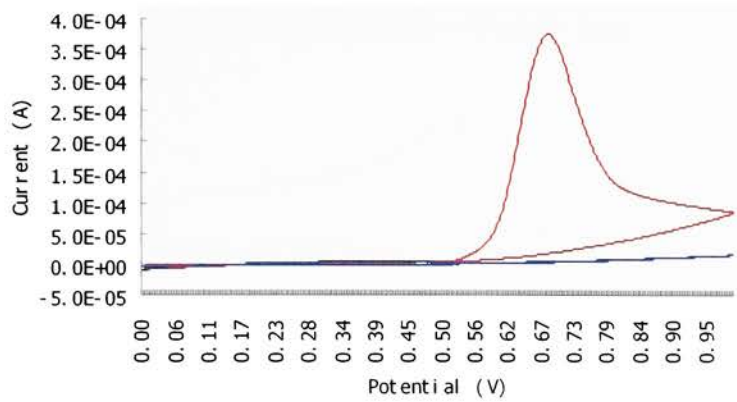

Figure 13. Electrochemical synthesis of polyaniline nanotubes. Cyclic voltammetry curve for aniline reduction in 0.1 N H_3PO_4 medium.

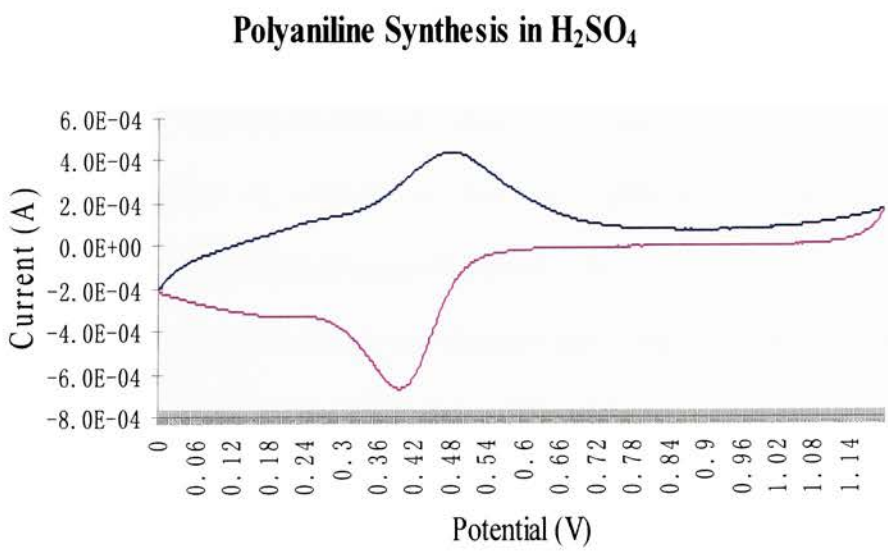

Figure 14. Cyclic voltammetry curve for a polyaniline film. Film characterization for electro-polymerized amorphous polyaniline on a Pt plate electrode.

In the nanotube film, there are clearly two distinct peaks in the first sweep (blue), one at 450 mV and one at 840 mV. These decay to form one peak in sweep 2 (red) at 530 mV which is almost identical to that of amorphous electropolymerized polyaniline films. It was therefore our observation that

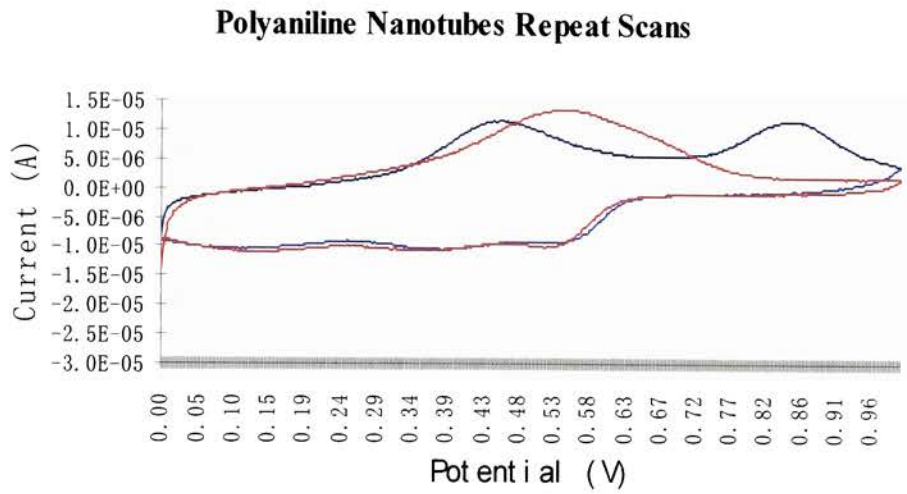

Figure 15. Cyclic voltammetry curve for a polyaniline nanotube film. Film characterization for electropolymerized polyaniline nanotubes on a Pt plate electrode.

the product of the electropolymerized emulsion reaction (polyaniline nanotubes) has another energy barrier in addition to that of traditional polyaniline to oxidation. Conformational restriction provides an explanation as to why this could be evident and it was indeed seen that no tubes were present after one sweep to 1200 mV potential. This provides further support to the idea that conformational restriction is the reason for nanotube formation rather than crystallization. It can also be ruled out that the additional peak is due to aniline monomer initiation. This is because the initiation peak (700 mV) and the unknown peak (900 mV) are at different potentials.

3.2.2 UV-Visible Spectroscopy

The spectra of our earlier prepared polyaniline nanotubes (Figures 5 and 6) were used to compare our newly electropolymerized material to. It was necessary to conduct this synthesis on indium-tin oxide enriched plastic so as to have a transparent medium to coat during electropolymerization for later UV-Vis characterization. Polyaniline nanotube film was again produced in 0.1 N H_3PO_4 medium. The film produced was washed and allowed to dry for 24 hours prior to spectral characterization. This spectrum is shown in Figure 16 (spectra of amorphous polymer were identical to spectra for nanotubes so they were omitted).

When comparing Figures 5 and 6 to Figure 16, it can be seen that the peaks at 440 nm and 880 nm are conserved indicating a conducting, or doped, state. This spectrum shows a more stable doped state than that of the chemically produced polyaniline nanotubes in that there is no peak present at 600 nm. This peak is indicative of exciton formation and is generally regarded as being less conductive than the presence of a bi-polaron which gives rise to the peak at approximatrly 900 nm.[12] Therefore, it can be concluded that electrochemically produced polyaniline nanotubes may be better candidates for electronics applications due to their more stable conductive state.

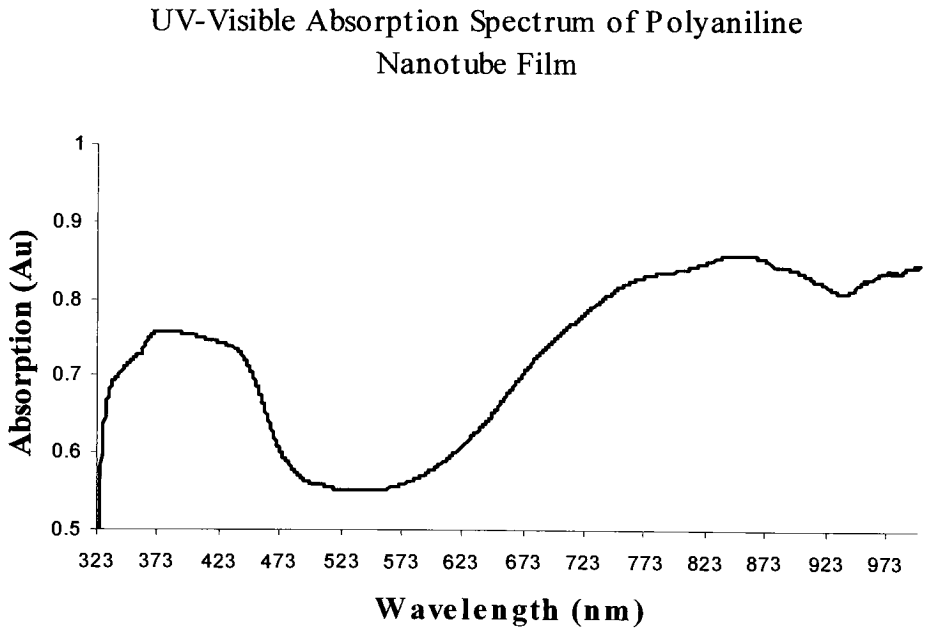

Figure 16. Visible spectroscopy of electrochemically produced polyaniline nanotubes. UV-Visible spectrum of polyaniline nanotube film produced by electropolymerization.

3.2.3 Diffuse-Reflectance FTIR

The same film used for UV-Vis qualification was used for FTIR analysis. The results of the electrochemically produced polyaniline nanotube film characterization are shown in Figure 17. Again, Figure 17 shows stark similarity to Figure 7 (the chemically produced polyaniline nanotube film) (again, amorphous polymer spectra were identical to spectra for nanotubes so they were omitted).

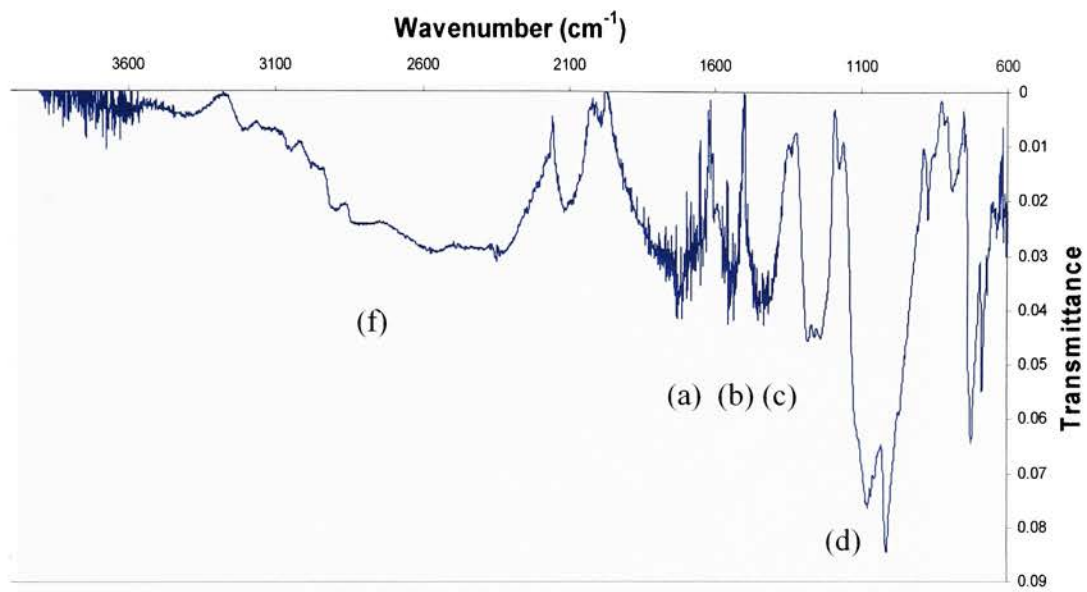

Figure 17. FTIR analysis of electrochemically produced polyaniline nanotubes. Diffuse-reflectance FTIR characterization of electrochemically produced polyaniline nanotube film.

3.2.4 Optical Microscopy

Films for both amorphous polyaniline and for polyaniline nanotubes were then examined by optical microscopy. Figure 18 shows an amorphous polyaniline film produced on a Pt plate electrode. There is no evidence of tubule formation in this micrograph. The film appeared ubiquitous and was well formed.

Figure 19 shows the polyaniline nanotube film produced on a Pt plate electrode. The absence of nanotubes in the amorphous film, Figure 18, was common to the entire film and conversely, the presence of nanotubes shown in Figure 19 was also representative of the entire plate. The tubules in this micrograph can be observed to

cluster to an extent. This was also observed over the rest of the plate. One reason for this could be from reorganization of the surfactant template particles in response to the application of current at the plate surface.

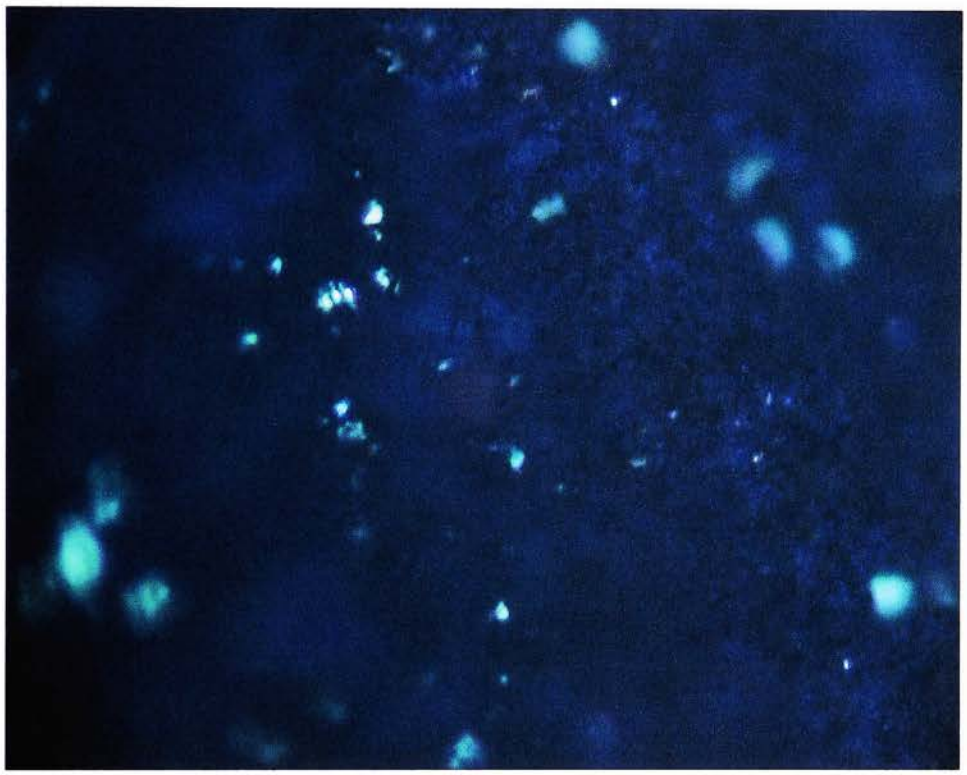

Figure 18. Amorphous polyaniline electrochemically deposited. Pt plate electrode.

The film produced on the ITO-enriched plastic is shown in Figure 20. This film also shows visual evidence of polyaniline nanotubes. The tubes produced on the ITO plate electrode were more well formed for the most part than they were using the platinum plate electrode. One reason for this was proposed that the plastic nature of the electrode (ITO coated plastic) may have helped facilitate the polymer particles attaching to the plate and remaining there whereas the metal platinum is slightly higher surface energy and therefore more difficult to adhere to.

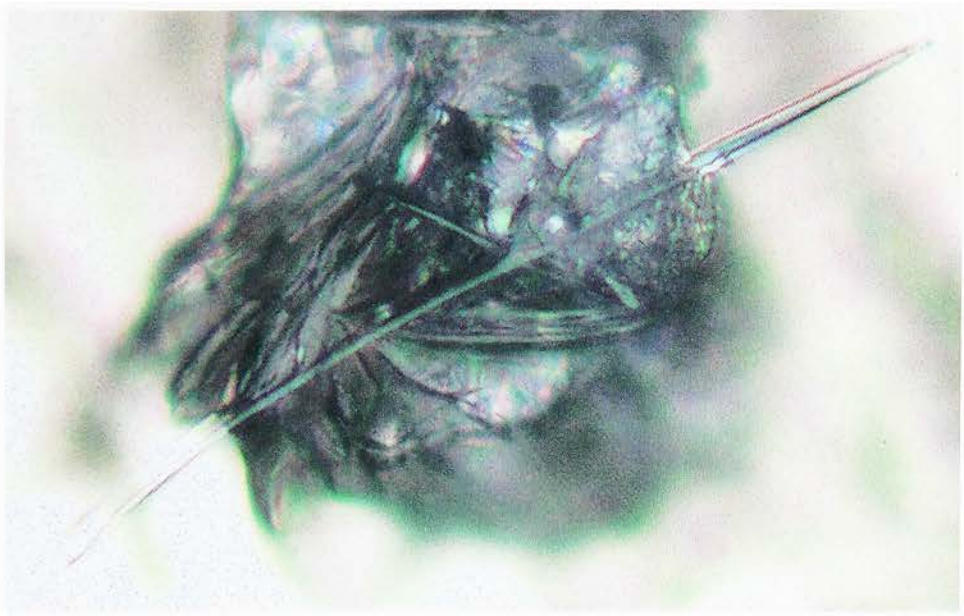

Figure 19. Polyaniline nanotube film electrochemically produced. Pt plate electrode.

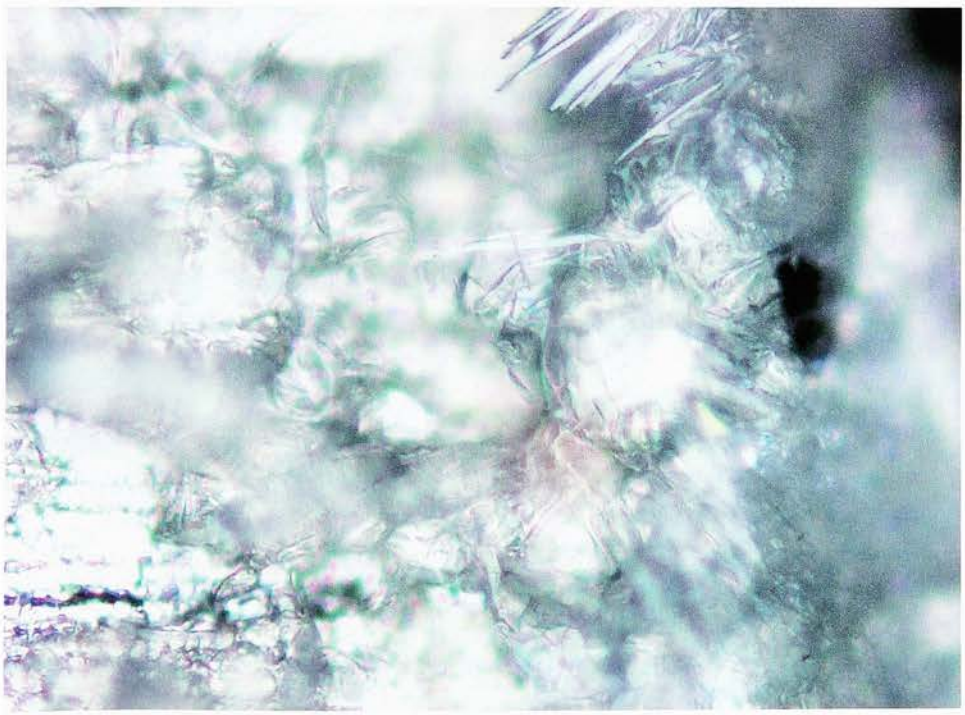

Figure 20. Polyaniline nanotube film electrochemically produced. ITO-enriched plastic electrode.

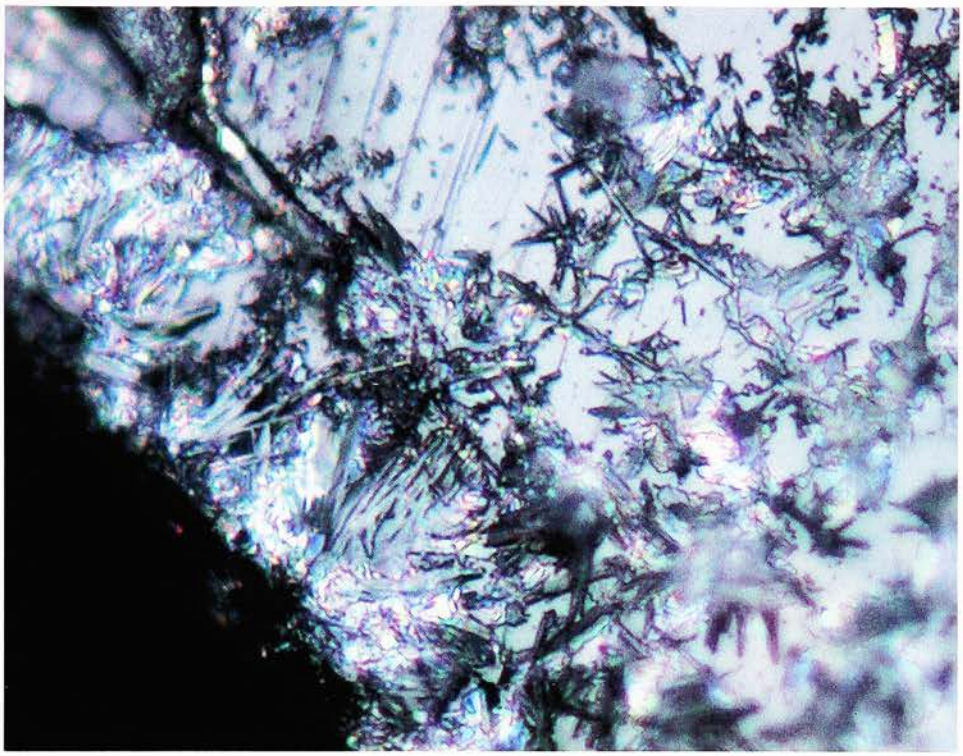

Figure 21. Polyaniline nanotube film produced on ITO-enriched plastic. Edge-on view.

Interestingly, it was noted that nanotube growth occurred most often at the electrode edges as shown in Figure 21 for the ITO electrode.

3.3 Polyaniline Nanotube Mediated Conversion of Aniline to Azobenzene

Next, we chose to determine whether or not polyaniline nanotubes could be used as catalysts for the oxidative conversion of aniline to azobenzene. This had already been demonstrated for functionalized carbon nanotubes.[30] Polyaniline nanotubes are roughly 10 times the diameter of functionalized carbon nanotubes so it was interesting to see if the larger diameter would have an effect on the reaction.

Oxidative conversion of aniline to azobenzene is a two-part oxidation. The reaction mechanism is show below in Scheme 2. In this reaction, aniline is oxidized to form nitrosobenzene initially. This is followed by another oxidation event to form the final product of azobenzene. This reaction unfortunately produces many undesired byproducts, one of which is azoxybenzene. For the catalysis using functionalized carbon nanotubes, little or no azoxybenzene was produced.

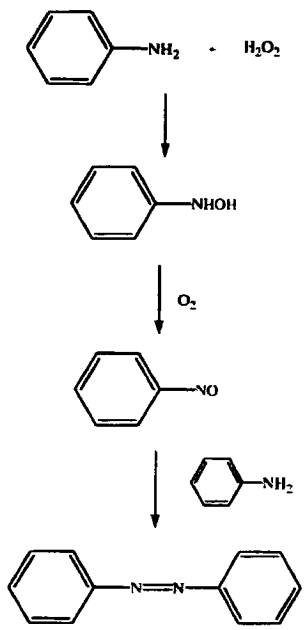

Scheme 3. Conversion of aniline to azobenzene by oxidation.

3.3.1 UV-Vis Timecourse Study of Aniline to Azobenzene Conversion

A time-course study of the catalytic behavior of polyaniline nanotubes for aniline to azobenzene conversion was then performed. The experiment utilized several controls: (1) no catalytic body present, (2) unfunctionalized multi-walled carbon nanotubes, and (3) amorphous polyaniline. Two active samples were also examined: (a) 3:1 emulsifier/monomer reaction product and (b) 4:1 emulsifier/monomer reaction product.

Aniline was oxidized to azobenzene by addition of 30% hydrogen peroxide to aniline monomer in acetonitrile medium with corresponding catalytic conditions. Azobenzene absorbs radiation at 327 nm and 425 nm characteristic of it's *cis*- and *trans*- forms. Figures 22 and 23 show the graphical results of monitoring absorption intensity at 327

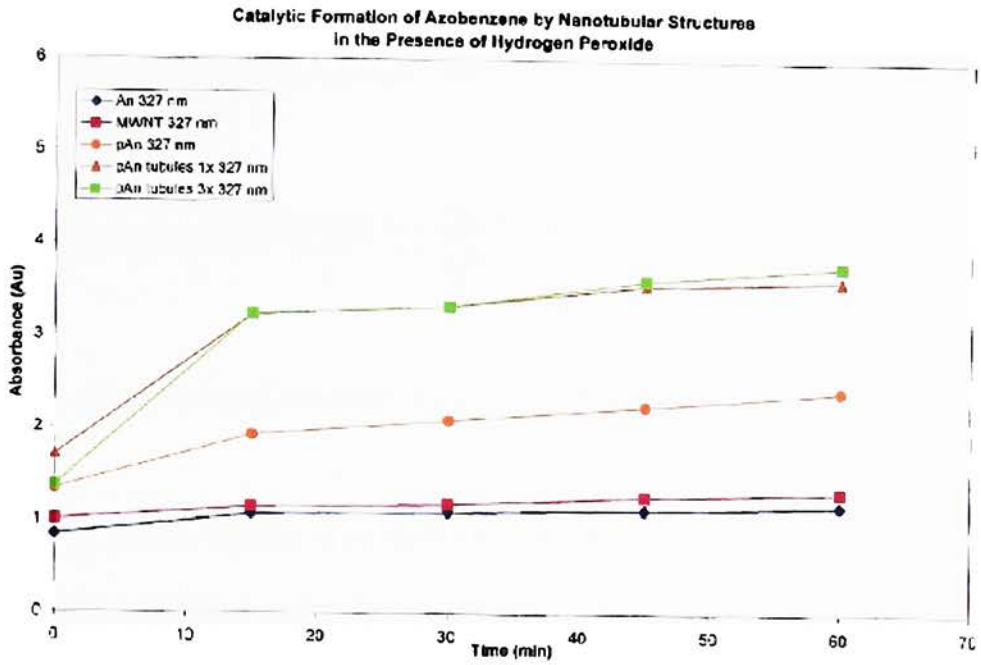

Figure 22. Time dependent absorption of *cis*-azobenzene (327 nm).

nm and 425 nm respectively. Catalytic behavior is demonstrated for polyaniline nanotubes in converting aniline to azobenzene in both the 3:1 and 4:1 samples. Figure 22 shows that polyaniline nanotubes produce the cis- form of azobenzene at different rates depending on the final morphololgy of the tubes. From Figures 9 and 10, it can be seen that morphology is affected by the surfactant/monomer ratio. This allows for more surface area both inside and outside of the tubes for 3/1 surfactant/monomer synthesis.

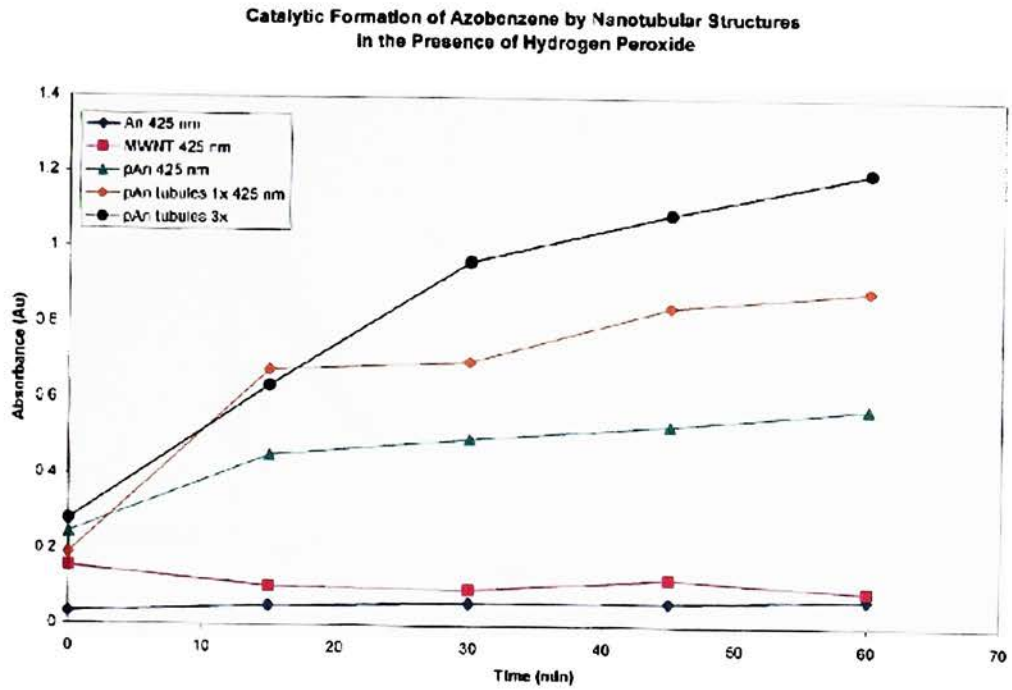

Figure 23. Time dependent absorption of *trans*-azobenzene (425 nm).

Whether or not the aniline to azobenzene conversion is taking place inside or outside of the tubes is not known at this time. Polyaniline demonstrates some catalysis for the *cis*-form of azobenzene as well when compared to controls.

Figure 23 shows a stronger catalytic effect for polyaniline nanotube mediated conversion of aniline to *trans*-azobenzene. There is a greater rate of azobenzene production in the polyanilne tubule enriched experiments. Furthermore, there is a product production rate enhancement for the 3/1 loading relative to the 1/1 loading. The reaction may also exhibit some stereospecificity. The likelihood that more of the *trans*-form is being produced because of kinetic conditions is higher however. The spectra were also taken at each time point and the 3/1 loaded sample is shown below in Figure 24.

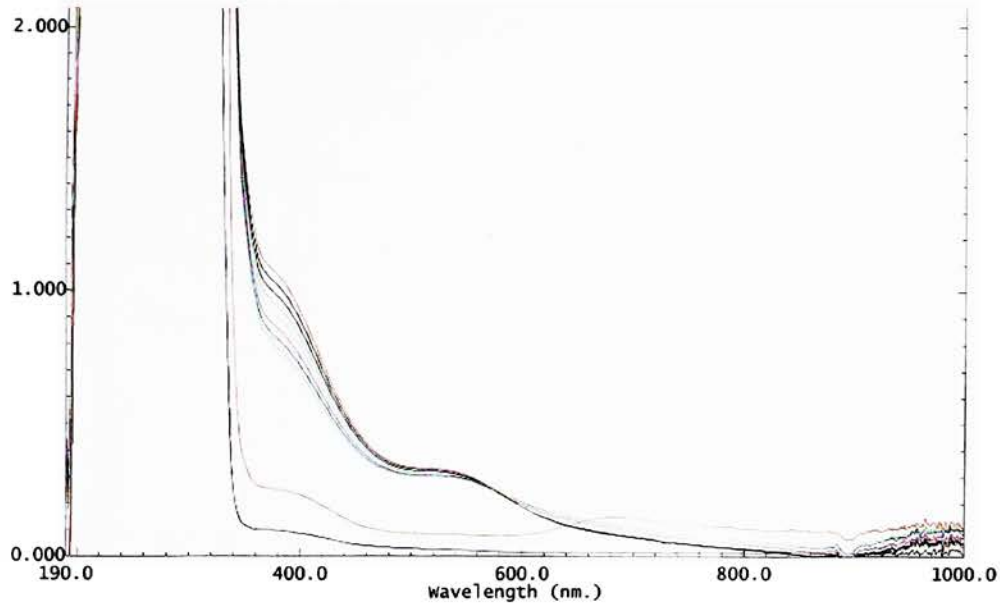

Figure 24. Time course study of polyaniline nanotube catalysis. Catalytic conversion of aniline to azobenzene by a 4:1 emulsifier/monomer reaction polyaniline nanotube product.

3.3.2 GC-MS Analysis of Aniline to Azobenzene Conversion

This provided qualitative evidence for polyaniline nanotube catalysis of aniline to azobenzene conversion. These results however, needed to be quantified. This was accomplished by monitoring the amount of azobenzene produced in an on column oxidation of aniline. Azobenzene production was monitored by GC-MS after 3 passes over a column packed with 100 mg of polyaniline nanotubes and glass fiber cap as compared to a control column of glass fiber only. The results of this experiment are shown in Figures 25 and 26.

In Figure 25, the molecular ion peak at 11.9 minutes is that of azobenzene and the peak at 13.2 minutes is that of the contaminant azoxybenzene. These values were measured against the monomer ion count peak (at 6.9 minutes) as an internal standard.

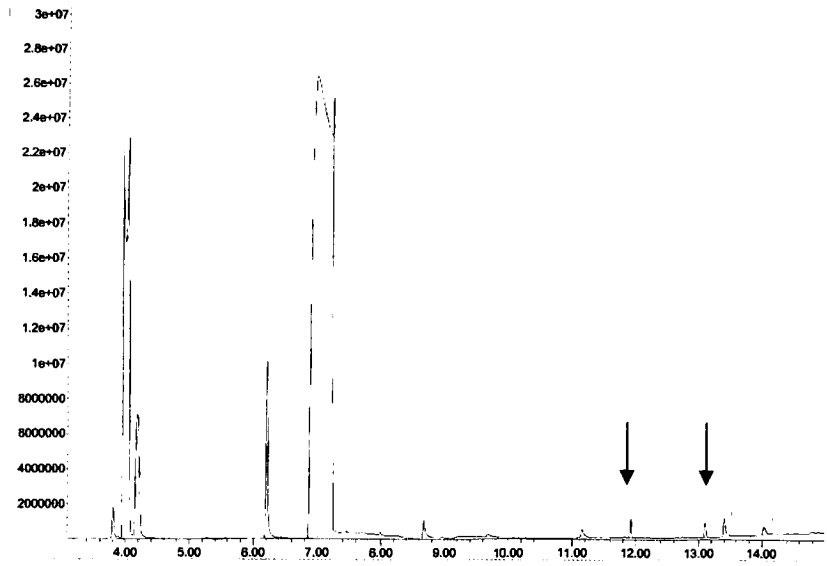

Figure 25. GC-MS ion count chromatogram. Catalysis of polyaniline nanotube on-column aniline to azobenzene conversion.

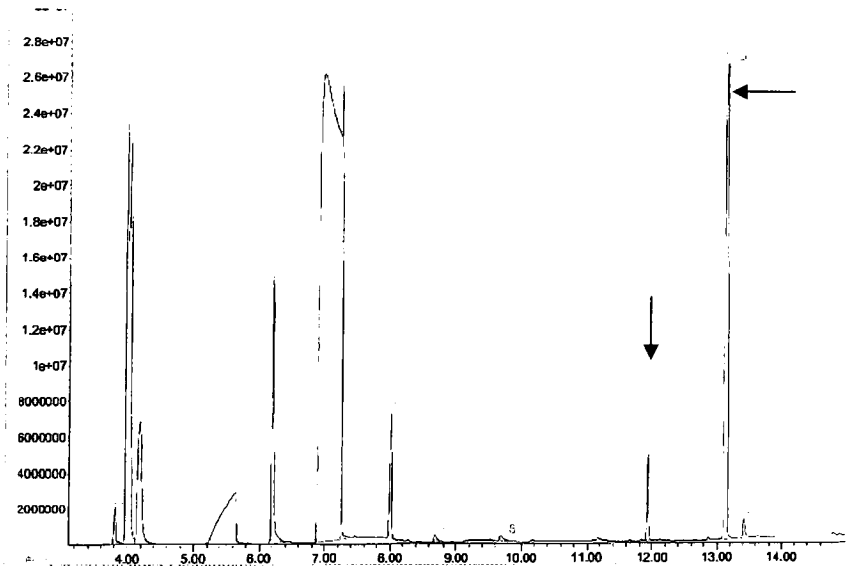

Figure 26. GC-MS ion count chromatogram. Control column aniline to azobenzene conversion.

As shown, the contaminant has roughly the same peak area as the desired product. In the control column experiment shown in Figure 26, there is a much larger peak for the contaminant than for the main product. The catalytic effect of polyaniline nanotubes on

the conversion of aniline to azobenzene results from suppression of the byproduct azoxybenzene from being formed.

The ratios of peak areas when compared for the two chromatograms result in the polyaniline nanotube column having a azobenzene/azoxybenzene ratio of 1.309 where in the control column a azobenzene/azoxybenzene ratio of 0.076 is observed from peak area counts. Therefore, polyaniline nanotubes show a catalytic enhancement of azobenzene production of 1722% versus control.

3.4 Thermal Conversion of Polyaniline Nanotubes to Carbon Nanotubes

As stated earlier, Kim and Jin have managed to carbonize poly(para-phenylene vinylene) (PPV) to form carbon nanotubes.[28] They did this by heating PPV nanotubes formed in templates to 1000°C. The tubules which resulted were found to be carbon nanotubes. This was the impetus for our group to test this idea on polyaniline. Polyaniline and PPV are very different polymers and this thermal conversion was found not to be as universally conserved as one might think. The main reason for this is that PPV requires some pyrolysis even to form. It must be heated to 800°C simply to form from a precursor. Polyaniline on the other hand can be formed at room temperature. The thermal properties of both polymers are very different as well with polyaniline having a thermal degradative transition by TGA at app. 500°C while PPV has a thermal transition by TGA at 800°C.[29] It was found that this may be profoundly important to the selection for particular carbonization products—such as single walled carbon nanotubes.

3.4.1 Thermal Gravimetric Analysis of Polyaniline Carbonization Products

The thermal properties of amorphous polyaniline and polyaniline nanotubes were examined by TGA. These are shown in Figures 27 and 28. Both TGA thermograms

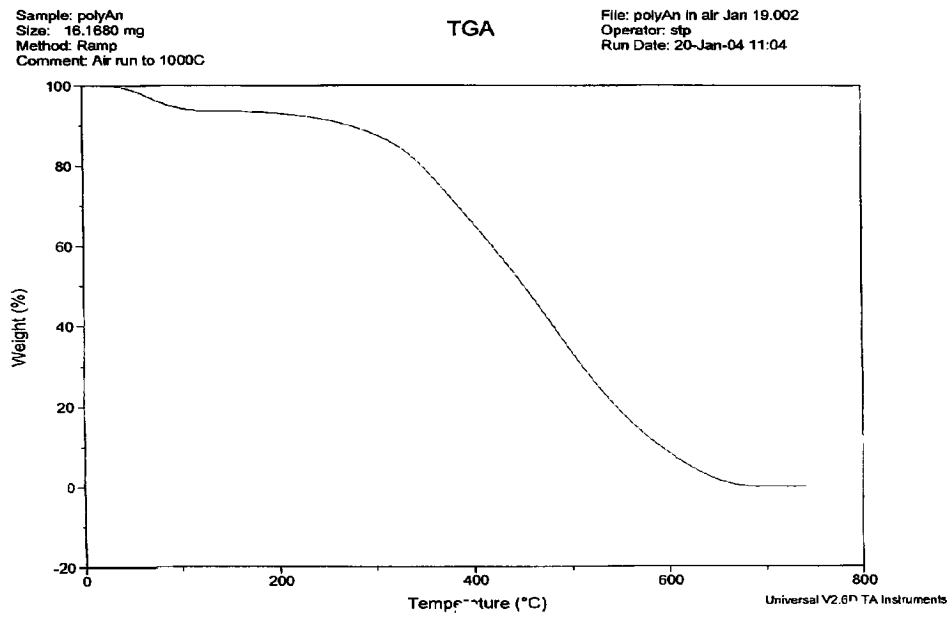

Figure 27. TGA of amorphous polyaniline in compressed air.

show a thermal transition at 500°C however, the polyaniline nanotube sample has an additional thermal transition at 350°C. This thermal transition must result from polyaniline nanotube thermal degradation since it does not occur in the amorphous sample. More interestingly, when heated in argon for 1 hour at 400°C, the polyaniline nanotube sample become devoid of tubular morphology and gives the TGA curve shown in Figure 29. Note this TGA curve has only one thermal transition at 500°C which is the same as that for the amorphous sample.

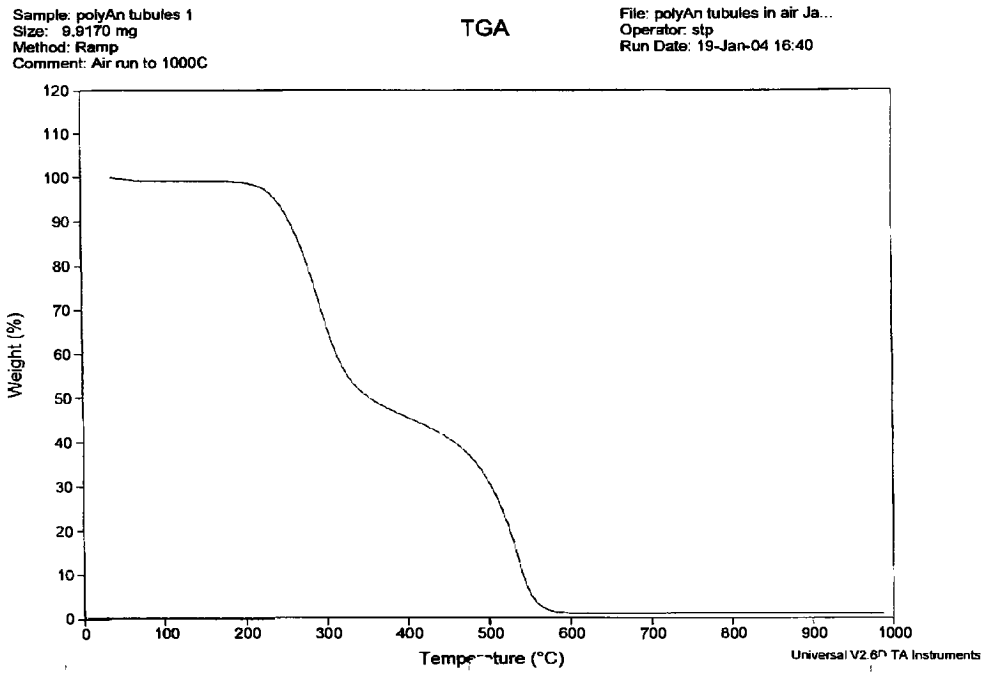

Figure 28. TGA of polyaniline nanotubes in compressed air.

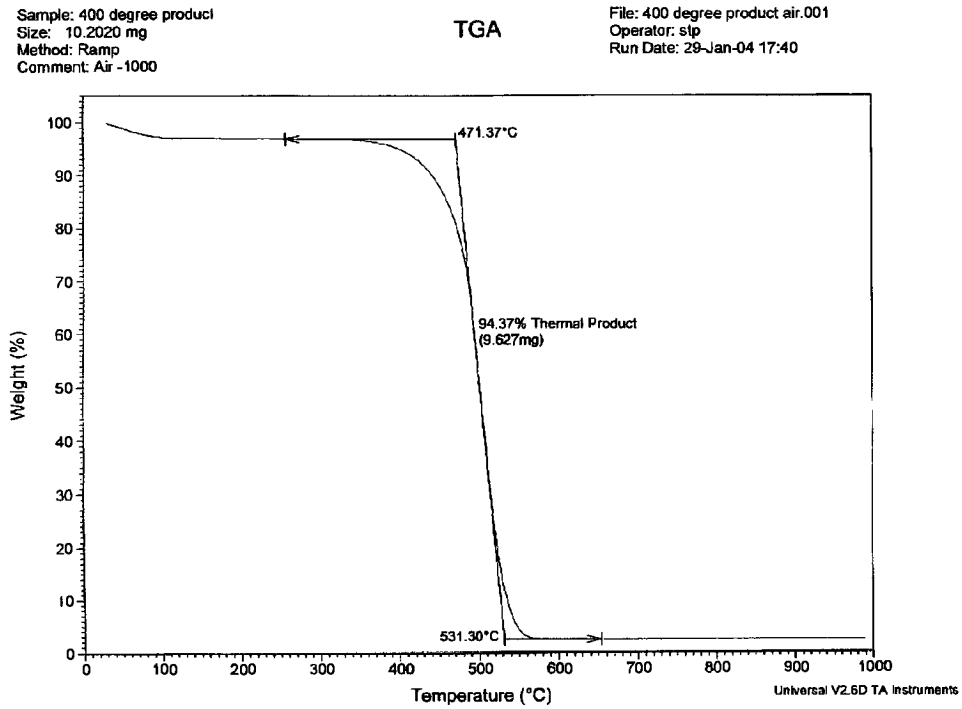

Figure 29. TGA curve for pre-heated polyaniline nanotubes (400°C for 1 hour).

3.4.2 FTIR Analysis of Polyaniline Thermal Carbonization Products

Diffuse-reflectance was used to examine the products of varied heat treatments on a polyaniline nanotube sample. This same sample was conserved throughout the experiment and was subjected for one hour to heat treatment in Ar(g) at 275°C, 400°C, and 1000°C. The results of these heat treatments are shown in Figure 30.

Two things are noteworthy here. The disappearance of the N-H stretching peak at 275°C and the continuous smoothing of the fingerprint region of the FTIR spectra past this temperature.

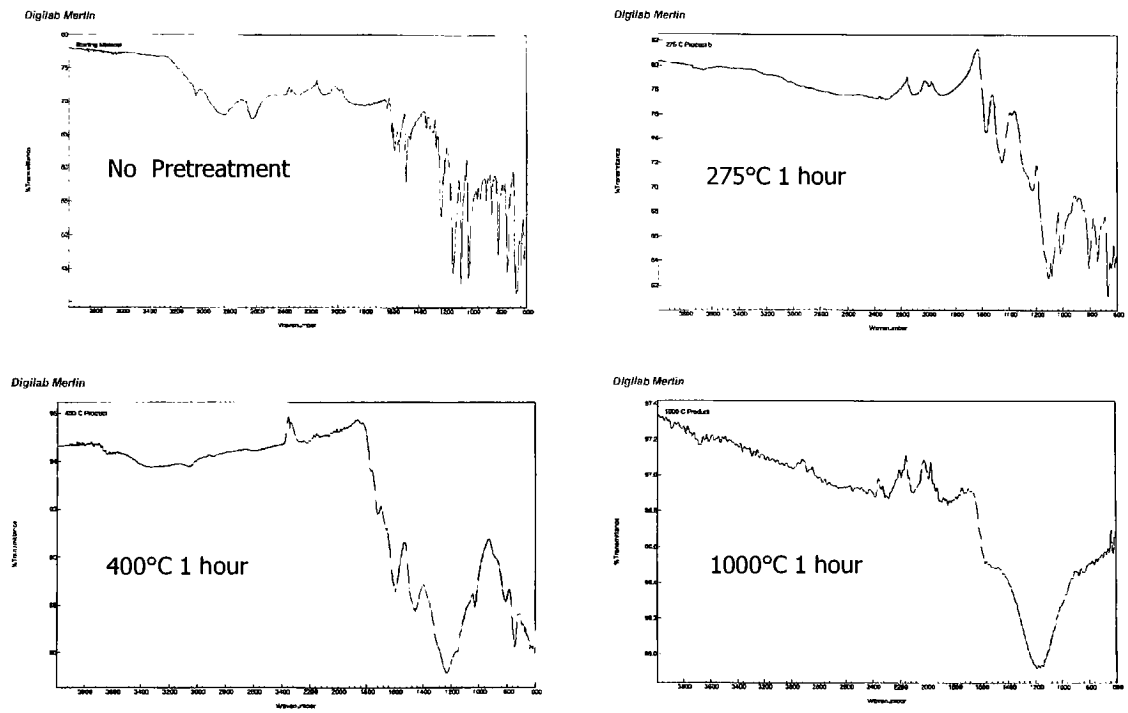

Figure 30. Heat treatment of a polyaniline nanotube sample. Sample treatment times are indicated in each FTIR spectrum

Firstly, the disappearance of the N-H stretch has important implications in that the structure of the parent polymer is being altered chemically. This loss of the N-H moiety

signifies that the tubule is being carbonized. Secondly, the loss of rotational and translational freedom shown by the smoothing of the absorption peaks in the fingerprint region means that the nanotube molecular structure is becoming more rigid. Both of these traits are common to MWCNTs[32]

3.4.3 EDX SEM Analysis of Polyaniline Thermal Carbonization Products

Figure 31 shows the micro-elemental analysis for the sample heated to 400°C. It shows complete loss of nitrogen. It also shows that the counter-ions from the dopant are still present (S and O) after 400°C heat treatment. This implies the first step in carbonization has occurred in that the parent structure has changed by losing all nitrogen.

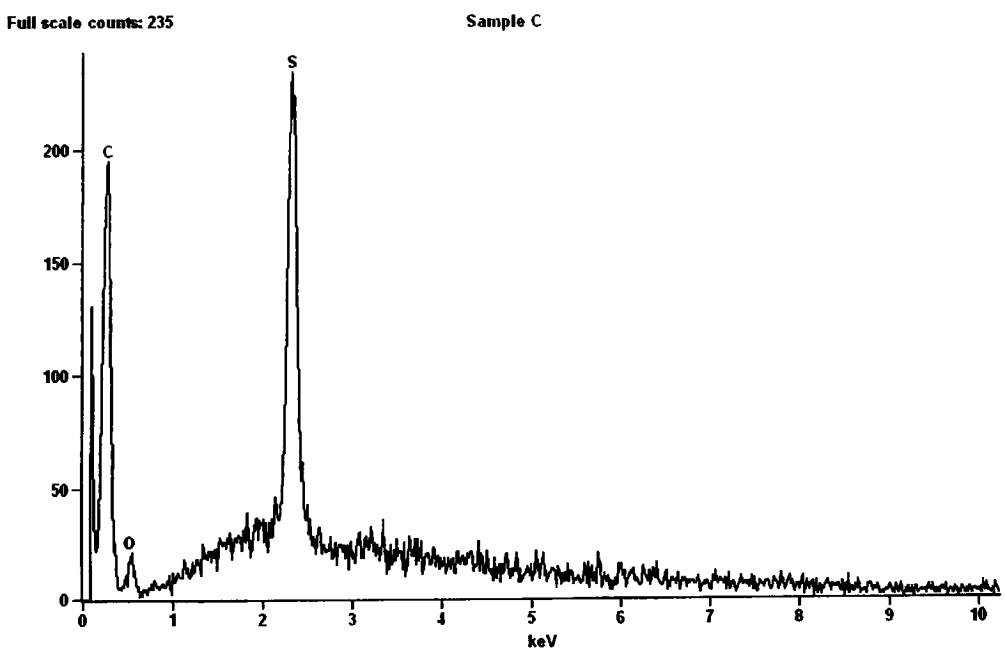

Figure 31. Elemental analysis of heat treated polyaniline nanotubes. EDX micro-elemental analysis of 400°C heat treated polyaniline nanotubes.

This is somewhat strange since the counter ion for the dopant sulfonyl group in the polymer, quinoid ammonia, has been lost already by both EDX and FTIR. One possible interpretation is that the dopant ion has been incorporated into the parent structure at this point. This does not disqualify these particles from being carbon nanotubes but simply that there may be defect centers in the tubes. This is commonly seen in carbon nanotube research that defects may give rise to attachment sites for grafting groups such as alkokyamine groups.[33]

Figure 32 shows the EDX micro-elemental analysis for the 1000°C heat-treated sample. It is evident from Figure 32 that no dopant remains and that the polymer has been fully converted to carbon. This is also confirmed by the FTIR data as it pertains to loss of nitrogen. This means that any particles remaining at this temperature are carbon therefore, a tubular structure must be a carbon nanotube or rod. The differentiation

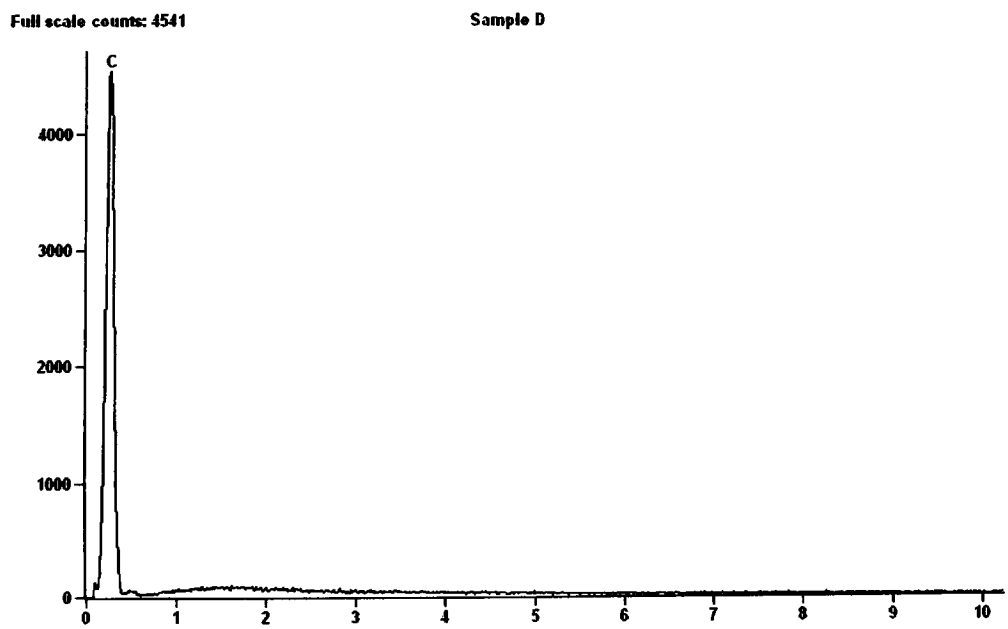

Figure 32. Elemental analysis of heat treated polyaniline nanotubes. EDX micro-elemental analysis of 1000°C heat treated polyaniline nanotubes.

between these two forms is not possible without TEM data for the case of multi-walled carbon nanotubes since the ends are capped. However, if one is present the other is also since there is no method to select for one over the other at this time using this method. The conformational restriction present due to the parent structures would, if anything, promote the formation of tubes over rods. The presence of amorphous material (rods) in the matrix of the heat produced carbon nanotubes was also shown by Kim and Jin.[28]

SEM imaging was then performed on these samples (Figures 33-36). Figure 33 is a really the same image as Figure 12. This was included here separately to give a sense of comparison. As is discussed earlier, tubular morphology is evident by the presence of an open ended body with round elongated shape. This sample was not heat treated and is therefore evidence of polyaniline nanotubes being present in the starting material.

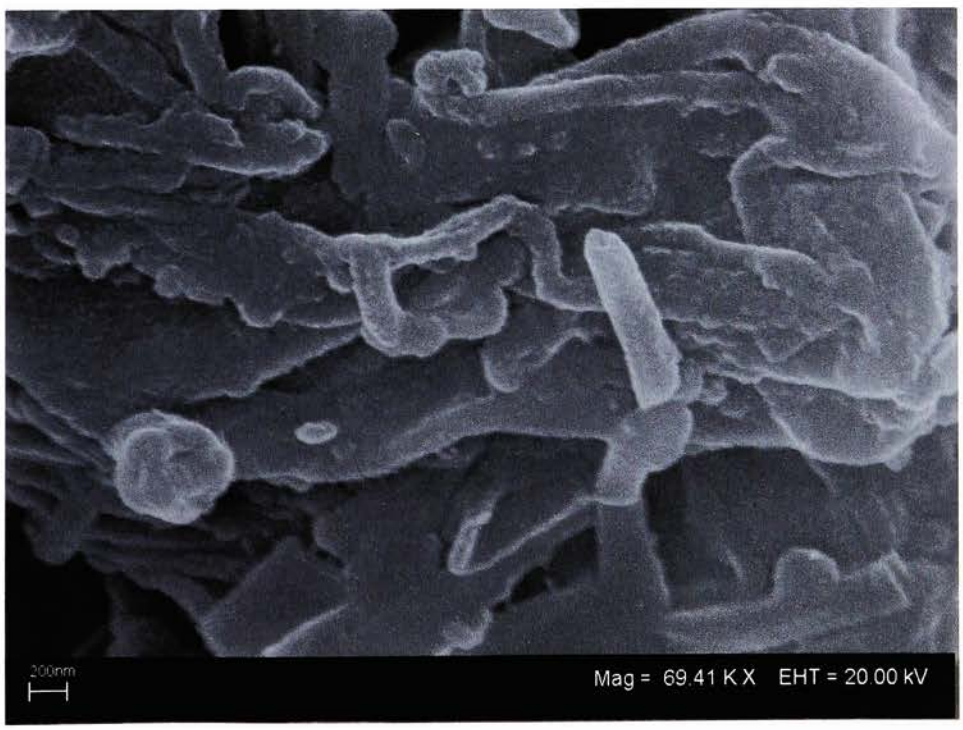

Figure 33. SEM Imaging of polyaniline nanotube sample. No pre-treatment was performed.

In Figure 34, a sample of the starting material after 275°C heat treatment for one hour is shown. An open ended structure is visible with round-elongated shape. This combined with the FTIR spectrum of this sample provide evidence of carbon nanotube formation. Whether or not traditional carbon nanotubes are formed by this method is unknown. Two things can be concluded from this image however: one that tubular structure is present, and two that the structures are open ended. Beyond this the only other thing which we are able to conclude is that the structures are carbon as verified by FTIR.

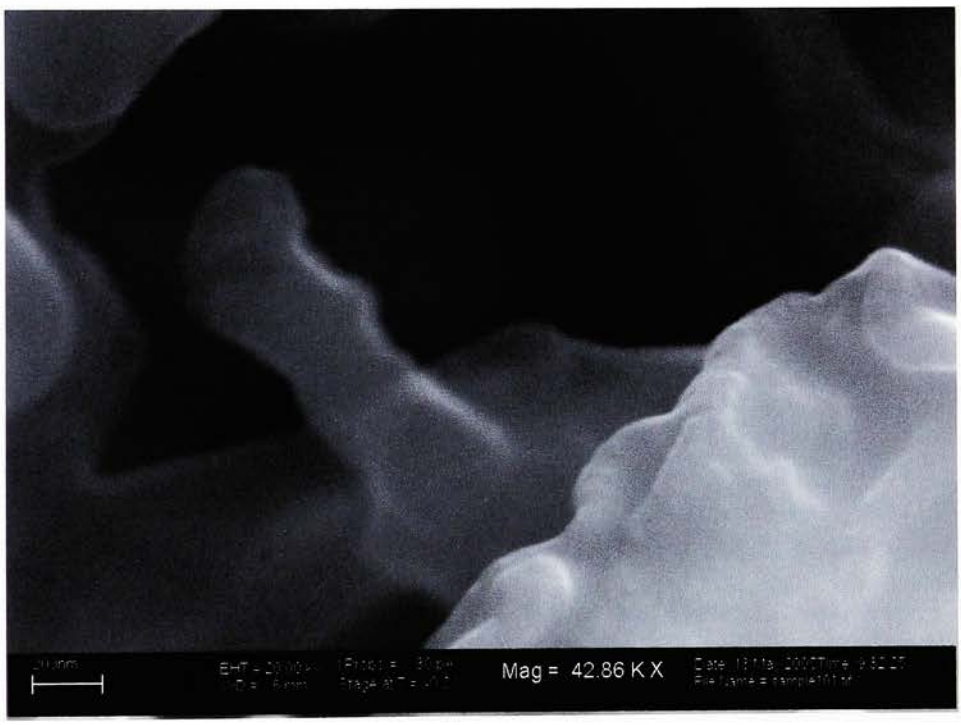

Figure 34. SEM Imaging of polyaniline nanotube sample. Pre-treatment at 275°C was performed.

Figure 35 is an image of a sample of the starting material after 400°C heat treatment for one hour. In this image, the tubular structures seem to collapse into the matrix material. This surface is also much more highly conductive evidenced by the

brighter color and better contrast of the SEM image. The sample took on a glassy texture during this heat treatment. It was therefore our theorization that the sample was being converted into glassy carbon above 400°C. No tubular structures were visible in this sample and none are seen in this image. The lack of tubules strengthened our position that polyaniline nanotubes were being thermally degraded at 275°C from the TGA curve data and led us further to believe that the sample was being converted to glassy carbon.

Figure 35. SEM Imaging of polyaniline nanotube sample. Pre-treatment at 400°C was performed.

The SEM image of the sample which was heat treated for one hour at 1000°C is shown in Figure 36. In this image clear tubular shape is observable. The ends are capped suggesting that this is possibly a multi-walled carbon nanotube. The sample at this point is completely converted to carbon by EDX analysis shown in Figure 32. Therefore, it can be concluded that carbon nanotubes may be produced by this method. An additional

thing to note is that this is not a neat conversion by any stretch. There is much amorphous carbon still in this sample however, it appears that small particulate species are almost completely tubular in shape.

Figure 36. SEM Imaging of polyaniline nanotube sample. Pre-treatment at 1000°C was performed.

4. Conclusions And Suggestions For Future Research

Polyaniline nanotubes have been successfully synthesized electrochemically for the first time without a template. This holds much promise to electronics applications as the need for better control over local environments expands with each generation of microchips. The polymer nanotubes produced by this method are not neat and would need some process refinement to benefit electronics industries however.

Polyaniline nanotubes have been shown to exhibit catalytic behavior for the conversion of aniline to azobenzene by suppression of the unwanted byproduct azoxybenzene inherent to the bulk reaction. Azobenzene is important as an azo-dye and it is advantageous and cost effective to large-scale production to create a more efficient synthesis. The suppression of synthesis by-products is one means with which to create a more efficient process. The ability to control for *trans-* vs *cis*-azobenzene production also appeared to have some merit in pursuing. It may be possible to choose which isomer to select for by altering synthesis conditions relative to the catalyst particles. This was not pursued in this thesis and may be interesting to follow up on.

Lastly, carbonization of polyaniline nanotubes at elevated temperatures has been shown to produce carbon nanotubes. This may take advantage of the pre-formed tubular shape of the polyaniline nanotube parent molecules. Whether or not this is occurring to form single-walled carbon nanotubes still needs to be investigated.

New ideas for research into this project would have to first include TEM data. The existence of the tubes is not in question but, some data on tube wall thickness as well as the number of wall layers produced at each temperature point on the TGA curve would benefit the project immensely. Another avenue of additional research that might be interesting could be to find an application for this concept. Perhaps forming carbon nanotubes in local environments from a precursor could be useful strengthening materials or in helping to facilitate polymer blend homogeneity.

One thing in particular that was not examined in this project which may be profoundly important in creating a bulk synthesis method for producing neat polyaniline nanotubes was the role of the surfactant particles in the electrochemical synthesis. It has

been shown that in fields of alternating current, micelles rearrange to form more ordered groups when adherent to a surface.[34] In this case the surface would be the working electrode and an alternation of current may be useful in selecting for purer samples of polyaniline nanotubes.

Other avenues of research are surely possible and I'm sure that some may be glaringly absent however, this work has shown 2 important things. First, that temperature control may be used to produce materials which would normally not be possible to make. By monitoring the TGA curve inflections carefully, one can select for a particular state to be populated. By controlling the dynamic between thermal degradation and static state, particular material states can be selected for. Secondly that by utilizing the faculties that surfactant particles lend to us, new and exciting methods for materials synthesis can be achieved.

5. References

1. Parthasarathy, R.V. and Martin, C.R. *Chemistry of Materials.* 6, 10, **1994**. 1627.
2. M. Wan Encyclopedia of Nanoscience and Nanotechnology. 2. **2004**. 153.
3. J. Huang, M. Wan, *J. Polym. Sci., A, Polym. Chem.* 37, **1999.** 151.
4. Alan J. Heeger. *J. Phys. Chem. B.* 105, 36, **2001**. 8475.
5. L. Dauginet-De Pra, S. Demoustier-Champagne, *Thin Solid Films*. 479, **2005.** 321-328
6. Allcock, H.R. and Lampe, F.W. Contemporary Polymer Chemistry: Second Ed. Prentice Hall, NJ. **1990**.
7. MacDiarmid, A.G.; Epstein, A.J. *Faraday Discussions of the Chemical Society.* **1989**. 88, 317.
8. Salaneck, W. R.; Lundstrom, I.; Haung, W. S.; MacDiarmid, A.G. *Synth. Met.* **1986**. 13, 291.
9. Cao, Y.; Smith, P.; Heeger, A. J. *Synth. Met.* **1992**. 48, 91.
10. Cao, Y.; Smith, P.; Heeger, A. J. U.S. Patent 5,232,631.
11. Burroughes, J. H.; Bradley, D. D. C.; Brown, A. R.; Marks, R. N.;Friend, R. H.; Burns, P. L.; Holmes, A. B. *Nature* **1990**. 347, 539.
12. C. Wang, Z. Wang, M. Li, H. Li, *Chem. Phys. Lett.* 341 **2001**. 431.
13. J.J. Langer, I. Czajkowski, *Adv. Mater. Opt. Electron.* 7, **1997**. 149.
14. J.J. Langer, *Adv. Mater. Opt. Electron.* 9, **1999**. 1.
15. Zhang, Z.; Wei, Z.; Wan, M. *Macromolecules*. 35, **2002**. 5937.
16. A.G. MacDiarmid, R.B. Kaner, in: T.A. Skotheim (Ed.), Handbook of Conducting Polymers, vol. 1, Skothim Marcel Dekker, New York, **1986**. p. 718.
17. Z.H. Wang, A. Ray, A.G. MacDiarmid, A.J. Epstein, *Phys. Rev., B.* 43, **1991**. 4373.

18. G. Gustafsson, Y. Cao, G.M. Treacy, N. Colaneri, A.J. Heeger, *Nature*. 357, **1992**. 477.

19. Dong, P.; Zhou, J.Z.; Xi, Y.Y.; Cai, C.D.; Zhang, Y.; Zou, X.D.; Huang, H.G.; Wu, L.L.; Lin, Z.H. *ACTA Physico-chimica Sinica*. 20, (5), **2004**. 54.

20. Fábio R. Bento and Lucia H. Mascaro. *J. Braz. Chem. Soc.*, Vol. 13, No. 4, **2002**. 502-509.

21. Yang, Y. and Wan, M. *J. Materials Science*. 12, 4, **2002**. 897.

22. Aydin,M., Arsu, N., Yagci, Y., Jockusch, S.,and Turro, NJ. *Macromolecules*. 38 (10): **2005**. 4133-4138.

23. L. Kelepouris and G. J. Blanchard. *J. Phys. Chem. B*. 106, **2002**. 6600-6608.

24. S. Iijima. *Nature*. 354 (6348): **1991**. 56-58.

25. Thostenson, E.T., Ren, Z., Chou, T.W. *Composites Science and Technology*. 61, **2001**. 1899-1912

26. Mindy Gordon. *Carbon Nanotube Catalysts: An Approach Toward Nanodimensional Reactions. Master's Thesis*. **2003**.

27. Takashi Kyotani. *Carbon*. 38, **2000**. 269–286.

28. Kim, K. and Jin, J.I. *Nano Letters*. 1, 11, **2001**. 631.

29. M. Croston, J. Langston, J. Tackacs, T.C. Morrill, M. Miri, K.S.V. Santhanam and P. Ajayan *Int. J. Nanoscience* 1, **2002**. 285.

30. Hongjin Qiu and Meixiang Wan. *Macromolecules*. 34, **2001**. 675-677.

31. Wan, M. X. *J. Polym. Sci., Part A: Polym. Chem.* 30, **1992**. 543.

32. Liu 1, M., Yang, Y., Zhu, T., Liu, Z. *Carbon*. 43. **2005**. 1470-1478.

33. Lou, X., Detrembleur, C., Sciannamea, V., Pagnoulle, C., Je´roˆme, R. *Polymer*. 45. **2004**. 6097–6102.

34. Ke-Qin Zhang and Xiang Y. Liu. *Nature*. 429. **2004**. 739-743.